CHALMERS
UNIVERSITY OF TECHNOLOGY

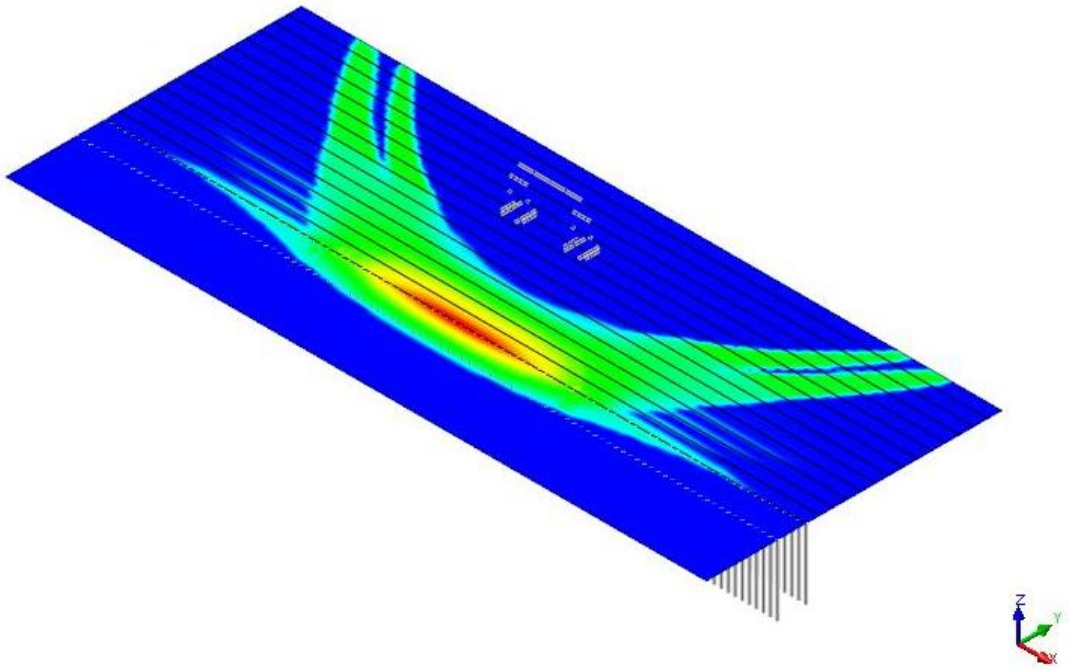

Structural assessment of concrete bridge deck slabs using FEM

Distribution of moments and shear forces

Master's Thesis in the Master's Programme Structural Engineering and Building Technology

Altaf Ashraf
Waleed Hasan

Department of Civil and Environmental Engineering
Division of Structural Engineering
Concrete Structures
CHALMERS UNIVERSITY OF TECHNOLOGY
Gothenburg, Sweden 2015
Master's Thesis 2015:143

MASTER'S THESIS 2015:143

Structural assessment of concrete bridge deck slabs using FEM

Distribution of moments and shear forces

Master's Thesis in the Master's Programme Structural Engineering and Building Technology

Altaf Ashraf

Waleed Hasan

Department of Civil and Environmental Engineering
Division of Structural Engineering
Concrete Structures
CHALMERS UNIVERSITY OF TECHNOLOGY
Göteborg, Sweden 2015

Structural assessment of concrete bridge deck slabs using FEM
Distribution of moments and shear forces

Master's Thesis in the Master's Programme Structural Engineering and Building Technology

Altaf Ashraf

Waleed Hasan

Examensarbete 2015:/ Institutionen för bygg- och miljöteknik,
Chalmers tekniska högskola, 2015

Department of Civil and Environmental Engineering
Division of Structural Engineering
Concrete Structures
Chalmers University of Technology
SE-412 96 Göteborg
Sweden
Telephone: + 46 (0)31-772 1000

Cover:
Maximum principal strain in the slab studied subjected to two concentrated loads as a result of non-linear FE analysis.

Printed by Chalmers Reproservice

Structural assessment of concrete bridge deck slabs using FEM

Distribution of moments and shear forces

Master's thesis in the Master's Programme Structural Engineering and Building Technology

Altaf Ashraf
Waleed Hasan
Department of Civil and Environmental Engineering
Division ofStructural Engineering
Chalmers University of Technology

ABSTRACT

Bridge deck slabs are critical to the load carrying capacity of bridges. The existing procedures often under-estimate the capacity of bridge deck slabs and therefore further investigation is needed to check if modern methods are more accurate. The aim of the project was to investigate the effect of redistribution of shear forces and bending moments on the load carrying capacity of bridge deck slabs subjected to point loads. The study also aimed at understanding the effect of parametric variations on the structural response of the bridge deck slabs.

A multi-level structural assessment method was adopted. The three different levels of assessment were simplified analysis, linear FE-analysis and non-linear FE-analysis. TNO DIANA was used to perform the FE-analysis of a cantilever bridge deck slab and results were validated by comparing them with the experiment performed by (Vaz Rodriguez 2007). Knowledge from previous master theses was also used in making certain modeling choices for the non-linear FE-model. For parametric studies, multi-level structural assessment was performed for each parametric variation. The results from each level of analysis were compared against that from the reference model.

The study showed that the methods of assessment normally used in engineering practice under-estimate the load carrying capacity of the slab. Improved methods, such as non-linear FE analysis, reflect the structural behavior of the slab better and also givea more accurate estimation of the load carryingcapacity of the structure. Results from this project showed that the recommendations in Model Code 2010 (CEB-FIP, 2013) over-estimated the one-way shear resistance of slabs, and therefore a new method was proposed that predicted the one-way shear resistance more accurately. The proposed method, however, requires further research for verification.

Parametric studies helped understand the impact of variations in different design and modelling parameters on the structural behavior. Support stiffness, effective depth, reinforcement ratio and influence of edge beams were the parameters that were studied. Each parametric variation changed the failure load of the slab. There was a significant change in distribution of shear forces in the slab when the support stiffness was reduced.

Keywords: FE-analysis, bridge deck slabs, parametric studies

Contents

Preface

The thesis focuses on non-linear finite element analysis of concrete bridge deck slabs. It was carried out at the Division of Structural Engineering, Department of Civil and Environmental Engineering, Chalmers University of Technology, Sweden. The thesis was started in January 2015 and ended in June 2015.

The master thesis was based on experiments performed by Vaz Rodrigues in 2007. The experimental results were used as a basis to evaluate the effectiveness of non-linear FE analysis in predicting load capacity of bridge deck slabs. Parametric studies were also performed to see the change in structural behavior of the slab when different parametric variations occur.

The thesis was supervised by PhD student Shu Jiangpeng and PhD KamyabZandi. The examiner for this thesis project was Associate Professor Mario Plos. We would like to thank them for their guidance and supervision throughout this project.

Göteborg August 2015

Altaf Ashraf & Waleed Hasan

Notations

Roman upper case letters

$C_{Rd.c}$	Co-efficient derived from tests
E_c	Modulus of elasticity for concrete
E_s	Modulus of elasticity for steel
M	Moment in a section of the slab
Q	Applied load on the slab for calculating the flexural strength
V_E	Applied load
$V_{Rd.c}$	One-way shear resistance
$v_{Rd.c}$	Punching shear resistance level I and level II analysis
V_R	Punching shear resistance level III analysis

Roman lower case letters

b_0	Perimeter of the critical section in punching shear
b_w	Distribution width
c	Length of the load application area
d	Effective depth
d_{g0}	Reference aggregate size
d_g	Maximum aggregate size
f_{ck}	Compressive strength of concrete
f_{ct}	Tensile strength of concrete
f_y	Yield strength of steel
k	Co-efficient dependent on effective depth of slab
κ_{dg}	Reference aggregate size
k_v	Constant dependent on the distance between reinforcement layers
l	Length of yield line
s	Constant
ν	Poisson's ratio
z	Center to center distance between top and bottom reinforcement

Greek letters

γ_c	Partial safety factor
ψ	Rotation of slab
α	Angel between yield lines of the slab
θ	Rotation at the support of the slab while calculating flexural strength

1 Introduction

1.1 Background

Bridge deck slabs are one of the most exposed bridge parts and are often critical for the load carrying resistance. The existing procedures for structural assessment often under-estimate the capacity of bridge deck slabs (Shu 2015). Consequently, it was important to examine the appropriateness of current analysis and design methods and see if modern methods provide more accurate results.

An important question was the distribution of bending moments and shear forces from concentrated loads. They were appropriately reflected in linear analysis, until the point where cracking occurs. Due to cracking of concrete and yielding of the reinforcement, these distributions change with increasing load, and a redistribution of linear moments will occurs. In engineering practice linear finite element analysis is often used in design as well as to predict the resistance of existing bridge decks. Since they do not reflect the real moments and shear force distribution accurately, redistribution of the linear moments and forces was needed.

1.2 Aim

The purpose of this project was to study the capability of existing design models for predicting the load carrying capacity of bridge deck slabs and to investigate the basis for further development of simplified models that could be used in assessment or design.The aim of the thesis was to use existing models and to evaluate their capability to show response and resistance of bridge deck slabs. The objectives of the project were to:

- Validate the modeling method for non-linear FE analysis with shell elements suggested by (Kupryciuk, Georgiev, 2013)using experimental results.
- Compare the load carrying capacity predicted with this modeling method to predictions with simplified methods for structural analysis.
- Study the distribution of moments and shear forces from non-linear and linear FE analysis.
- Investigate the effect of different parameters on the moment and shear force distribution through a parametric study.

1.3 Method

The method used in this project was to make a limited literature study and to perform analytical and numerical analysis. The results of the analysis were evaluated by comparisons to structural tests found in the literature. A parametric study was performed to study the influence on the results from different design parameters.

To achieve the aim, the distribution of moments and shear forces was studied with non-linear finite element (FE) analysis. The modeling method developed in a previous master theses(Kupryciuk, Georgiev, 2013)was used. The first step was to validate this method by comparisons tests previously performed by (Vaz Rodriguez 2007).

Critical sections of the bridge deck were identified and non-linear FE analysis was performed to study the distribution of shear and moment. The results from the non-linear analysis were compared with the corresponding distributions from linear FE analysis.

Structural analysis on three levels of was used to investigate the structural capacity of a cantilever bridge deck slab(Shu 2015). In level I, simplified methods, such as the strip method(Hillerborg 1996) were used in combination with resistance models from(Eurocode 2004). In level II a linear FE analysis was performed and combined with the same resistance modelsas for level I.In level III, a non-linear analysis was performed of the slab using resistance models fromModel Code 2010 (CEB-FIP, 2013).

A parametric study wasthen performed. Parameters including geometry, boundary conditions and load cases were changed to study their influence on the shear and moment distribution.

1.4 Limitations of the project

This master thesis was limited to the study of cantilever slabs only and just slabs without shear reinforcement. Thus the conclusions from the thesis are applicable to cantilever slabs without shear reinforcement only. In the FE-model of the slab, only shell elements were used. Use of other types of elements was not investigated.

2 Literature study

For this master thesis a limited literature study was performed which focused specifically on the experiments that could be used for verification of the modeling method. The literature study also included the previous master theses performed within the same research project at Chalmers. The experiment chosen was the one conducted by(Vaz Rodriguez 2007) at EPFL in Lausanne. The previous master theses studied were (Hakimi 2012) and (Kupryciuk, Georgiev, 2013). In the previous master theses projects, the same test(Vaz Rodriguez 2007) was used.

2.1 Tests on cantilever bridge deck slabs

Six tests were performed on two cantilever bridge deck slabs without shear reinforcements(Vaz Rodriguez 2007). The two slabs were referred to as slab DR1 and slab DR2. Three tests were performed on each slab. In each test the slab was subjected to a different load configuration. Out of the six tests performed, three were used in this thesis project. In the three tests that were used in this master thesis, the slab was referred to as DR2-A, DR2-C and DR1-A respectively in each test.

Both slab DR1 and DR2had a total length of 10 m and a transversal span of 4.2 m, see Figure 1.They had a uniformly varying cross sectional thickness, from 380 mm at the support to 190 mm at the free end.

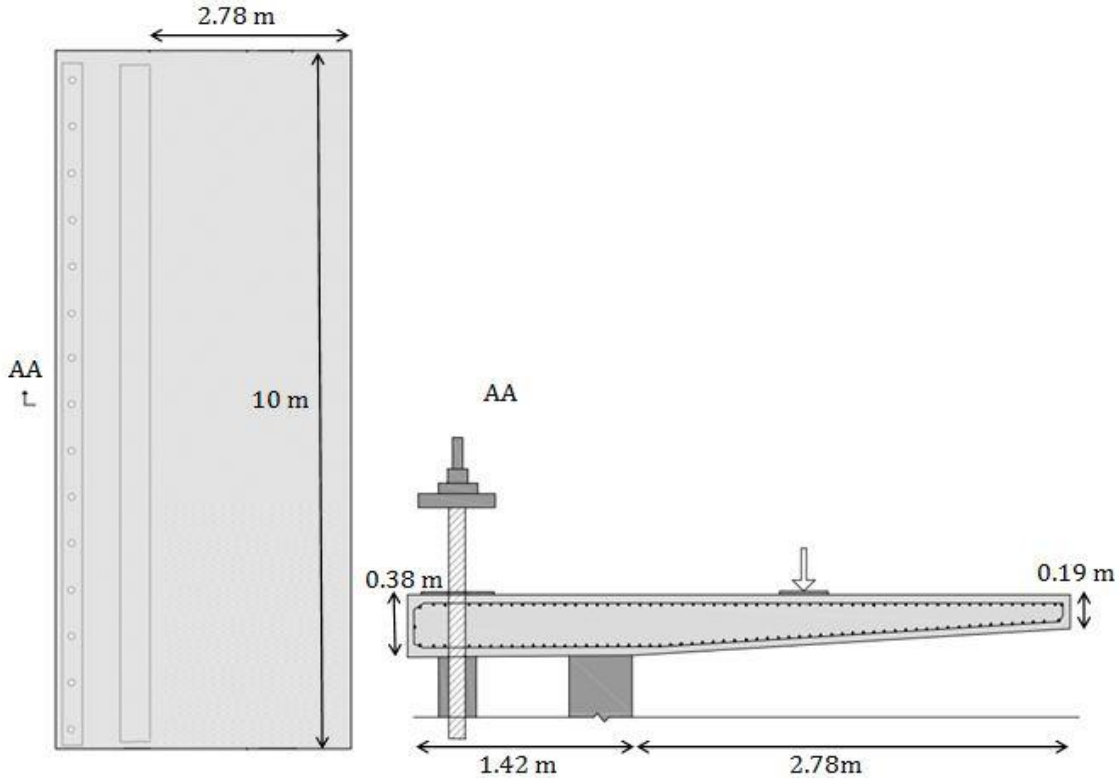

Figure 1 Geometry of slab DR1 and DR2, adopted from(Vaz Rodriguez 2007).

2.1.1 Test set-up

The two specimens had different reinforcement ratios and the reinforcement layouts as seen in Figure 2. For slab DR1,the main reinforcement in the top layer, in the cantilevering direction, consisted of 16 mm diameter bars with 75 mm spacing (reinforcement ratio $\rho = 0.79\%$). Every second bar was curtailed and only half of the reinforcement continued to the free end. The top reinforcement in the direction along the cantilever support consisted of 12 mm diameter bars with 150 mm spacing. The bottom reinforcement consisted of 12 mm diameter bars with 150 mm spacing in both directions. No shear reinforcement was provided in the specimen.

For slab DR2, the transversal reinforcement of the top layer consisted of 14 mm diameter bars with 75 mm spacing at the fixed end (reinforcement ratio $\rho = 0.6\%$).Similar to the slab DR1, every second bar was curtailed and only half of the reinforcement continued to the free end. The top reinforcement in the longitudinal direction as well as the bottom reinforcements were the same in both the specimens, See Figure 2.

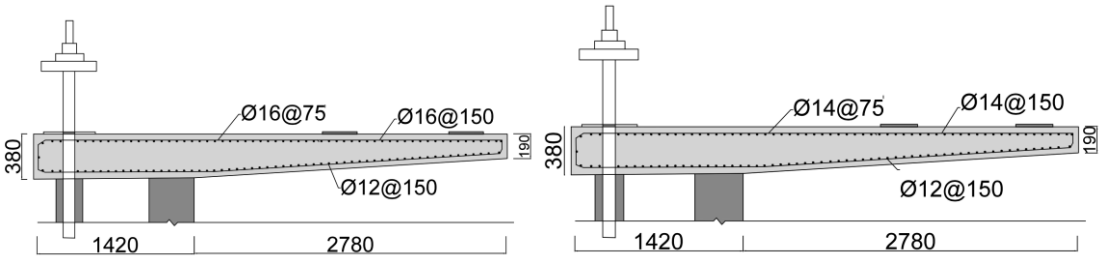

Figure 2 Reinforcement arrangement in slab DR1 and DR2, adopted from(Vaz Rodriguez 2007).

The fixed end support for the cantilever slab was obtained by supporting it on concrete blocks along the support line and clamping the rear end by means of vertical pre-stressing (7 MN total force), see Figure 2.

2.1.2 Load cases

Three load cases that were studied in this thesis. The slab is referred to as slab DR2-A, DR2-C and DR1-Afor each of the three cases considered. Figure 3 shows the load configurations all the six tests performed in (Vaz Rodriguez 2007). The three tests used in this thesis are highlighted in Figure 3.

Figure 3 *The six tests performed by (Vaz Rodriguez 2007) . Tests DR2-A, DR2-C and DR1-A were used in this master thesis and the encircled in the image above, adopted from (Vaz Rodriguez 2007).*

In slab DR2-A,two point loads were applied on an area of 300 x 300 square millimeters. The loads had a center to center distance of 900 mm between them and were at a distance of 1.3 m from the fixed support. .

The loading on slab DR2-A was applied in different stages. A load of 698 kN was applied in four stages and then the slab was unloaded soon after. The slab was loaded to failure after a gap of 12 hours with the total value of the load applied being 961 kN. Due to the pre-loading of the slab, the slab had possibly cracked before the final loading. The supporting concrete blocks were possibly compressed due to the pre-loading and might have lost their stiffness.

In slab DR2-C,one point load was applied on an area of 300 x 300 square millimeters. The load was at a distance of 1300 millimeters from the clamped support.

In slab DR1-A,four point loads were applied, with each load applied on an area of 300 x 300 square millimeters. For detailed descriptions of the tests refer to (Vaz Rodriguez 2007).

2.2 Previous master theses

Previous master thesisprojects by (Hakimi 2012) and (Kupryciuk, Georgiev, 2013) were also studied to get an understanding of the behavior and the finite element modeling of cantilever slabs under point loads.

The previous master theses focused on the shear distribution after the formation of cracks in the case of four concentrated loads (test DR1-A). The slab test used in both these projects is the same as one of the tests being analyzed in this master thesis, that is (Vaz Rodriguez 2007).

The choices made in the previous master theses regarding modeling of the slab in DIANA and the analysis procedures were carefully studied. To undergo a deformation controlled analysis, a loading substructure was employed, so that all the nodes that were being subjected to loading experienced the same load magnitude. Figure 4 shows the loading sub-structure used in this project.

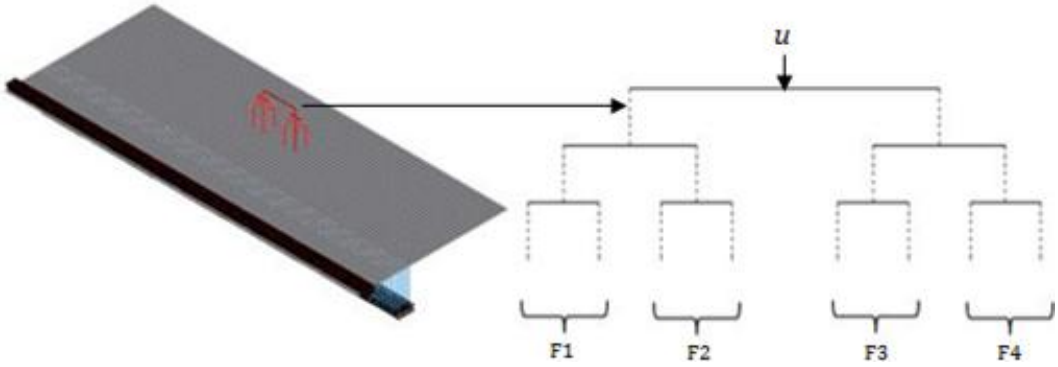

Figure 4 The loading substructure used in this project.

When modelingthe slab, the cantilever part was modeled as segments, with each segment having its own thickness (Hakimi 2012). This was done because a constantly varying shell thickness combined with inclined reinforcement members was not giving accurate results (Hakimi 2012). Figure 5 illustrates the modeling as done in this master thesis.

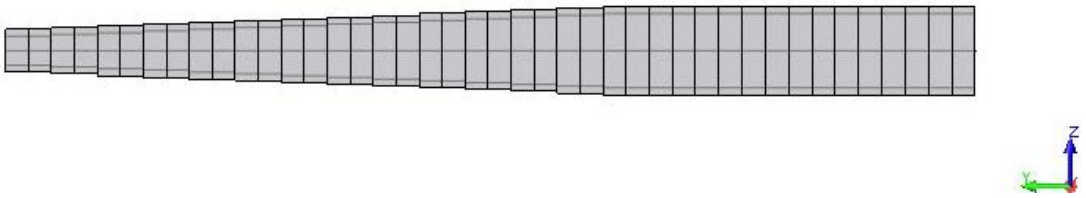

Figure 5 Modeling of the slab as segments as done in this project. This modeling was based on the suggestions in(Hakimi 2012).

In order to get a stable and reliable results in terms of shear distribution after the formation of cracks, it was suggested by (Kupryciuk, Georgiev, 2013) to use a higher order elements with a reduced integration scheme (8 nodes, 2x2x9).It was also observed that analysis carried out with poisons ratio ν=0 yielded better results in terms of shear fluctuations at the support region(Kupryciuk && Georgiev 2013). The same modeling choices were thus made in this master thesis as well.

3 Structural Analysis

For the assessment of the structural response of the concrete bridge deck slabs studied, a multi-level structural assessment method was used, as proposed by *(*Plos *et al* 2015). In this study, analysis was carried out in three levels of assessment as listed below.

- Level I: Traditional or simplified method.
- Level II: 3D linear FE analysis.
- Level III: 3D non-linear FE analysis.

The multi-level assessment system is illustrated in the Figure 6:

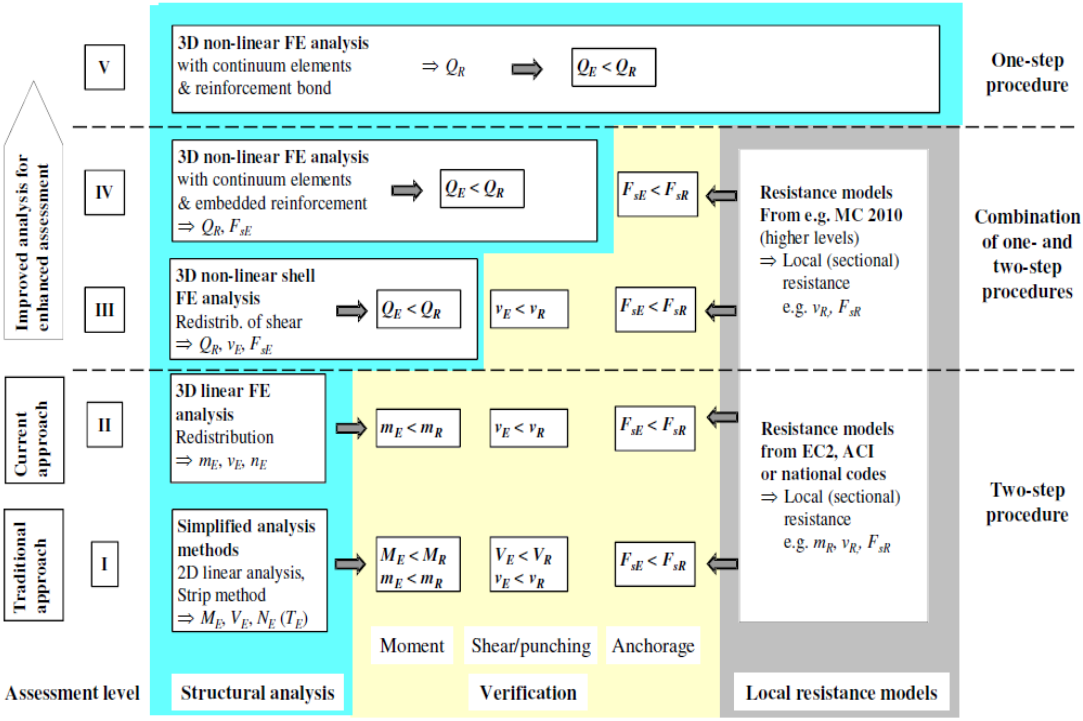

Figure 6 Themulti-level structural assessment system followed in this thesisproject, from(Plos et al 2015).

Each level provided a higher level of accuracy for structural assessment. For level I analysis resistance models from (Eurocode 2004)were used for evaluating the shear resistance of the slab. For level II, a linear FE analysis was performed and the results were checked against the resistance models from (Eurocode 2004). For level III, a non-linear FE analysis of the slab was performed and the results were checked against the resistance models from Model Code 2010 (CEB-FIP 2013). For level I analysis the flexural resistance of the slab was evaluated using yield line method.For level II analysis the flexural resistance was obtained using linear FE analysis. For level III analysis the flexural resistance of the slab was determined by checking the strain value that caused rupture of reinforcement in non-linear FE analysis.

3.1 FE modeling and analysis of the slab

For the multi-level structural assessment system, both linear and non-linear FE-analysis was performed. The following section describes the various modeling choices made for the analysis.

3.1.1 Element type

The element type to use depended on what type of response and failure the model should describe (Broo *et al* 2008). Since the aim of the thesis was to describe the redistribution of shear forces after the formation of bending cracks and moment redistribution due to cracking, the choice of curved shell elements was adequate (Kupryciuk, Georgiev, 2013). An illustration of a curved shell element with in plane forces and out of plane forces is shown in Figure 7.

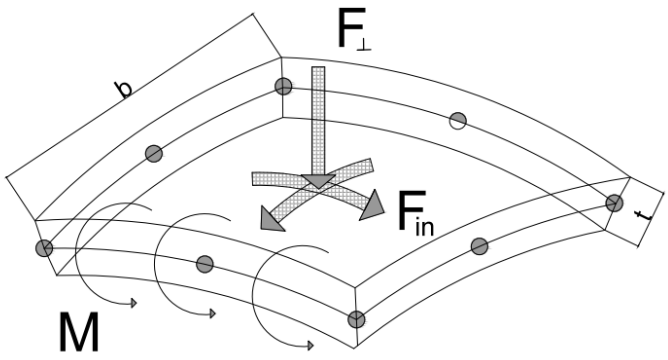

Figure 7 Curved shell elements, adopted from (TNO DIANA User manual realease 9.4.4 2011)

Although shell elements could not describe shear cracking nor shear failure for out of plane shear, cracking and failure for in plane shear could be described (Broo *et al* 2008). Hence, for shear failure, out of plane shear stresses were investigated for different values of loads until the value did not exceed the shear resistance of the reinforced concrete section using a separate resistance model.

3.1.2 Interaction between concrete and reinforcement

For the analysis, the embedded reinforcement approach was used(TNO DIANA User manual realease 9.4.4 2011). Full interaction between reinforcement bars and surrounding concrete was ensured by coupling the strains and displacements of their respective elements. The reinforcement elements did not have any degree of freedom of their own, and by default the reinforcement strains were computed from displacement field of the mother (concrete) elements(Broo *et al* 2008). A perfect bond existed between the reinforcement and the concrete and hence the structure was not analyzed for anchorage failures.

3.1.3 Material models

A linear relationship was assumed between stress and strain for linear analysis. Based on this assumption, simple isotropic models were chosen for both concrete and steel. The material parameters used for linear as well as non-linear analysis are shown in Table 1.

Table 1 Material parameters for linear analysis(Vaz Rodriguez 2007).

Parameter of concrete		Parameter of reinforcement steel	
Elastic Modulus	36.0 GPa	Elastic Modulus	200 GPa
Poisson's ratio	0.2(0)	Poisson's Ratio	0.3
Compressive strength	40 MPa	Yield Strength	515 MPa
Tensile Strength	3 MPa		

The non-linear behavior of concrete was represented using different material models available within(TNO DIANA User manual realease 9.4.4 2011). In this master thesis, concrete was modeled using a total strain rotating crack model. To define the behavior of concrete in compression and tension, (Thorenfeldt 1987)and (Hordijk 1991) stress-strain curves were used in the analysis respectively. The stress-strain behavior of concrete in each of these two models is show in Figure 8.

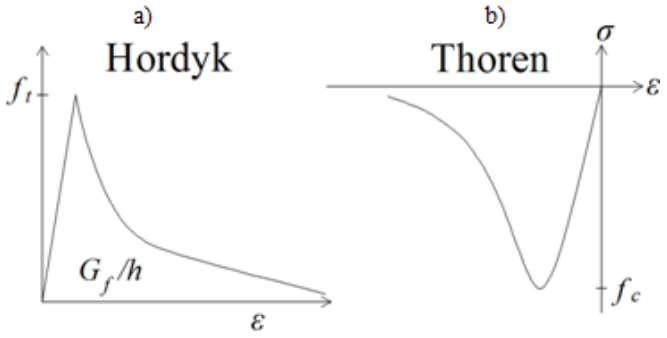

Figure 8 Material models for concrete a) In tension b) In compression, both figures areadopted from(TNO DIANA User manual realease 9.4.4 2011).

The analysis in this project was done using the smeared crack approach. The crack bandwidth was assumed as the mean crack distance and it was calculated to be 86mm based on the recommendations from (Eurocode 2004). For calculations see Appendix C. The fracture energy was calculated to be 64 Nm/m^2according to the Model Code 1993(Ceb-Fip 1993)based on the concrete compressive strength and the maximum aggregate sizes used in the test specimens.

3.1.4 Boundary condition

In the FE model, non-linear springs were used to model the support given by concrete blocks in the tests, as shown in Figure 9. The springs had a very high stiffness in compression but no stiffness in tension in order to account for possible uplift wherever required. The boundary conditions applied on the spring were such that the translations in x, y and z direction were fixed.The fixed end of the slab was also modeled by locking the translations in x, y and z direction.

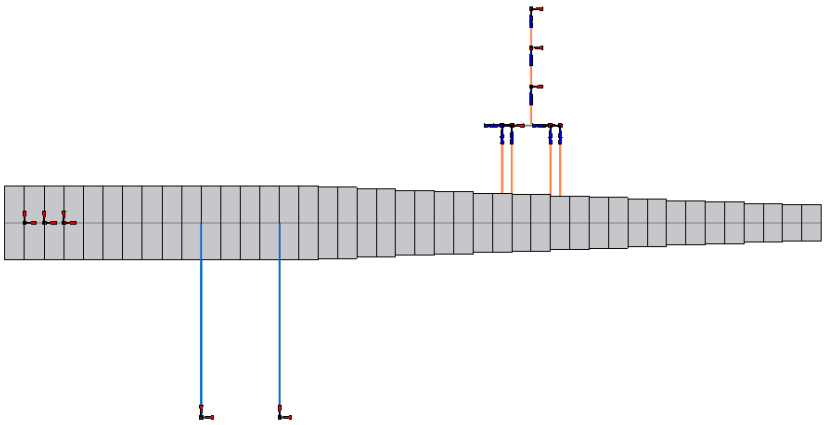

Figure 9 *FE-model showing the support conditions. Springs represent the concrete member that supported the cantilever part in the experiments.*

3.1.5 Mesh sizes

The bridge deck slab was meshed with quadrilateral curved shell elements of size 0.1 x 0.1m. A convergence study was performed in a previous master thesis (Hakimi 2012) with finer mesh sizes and it was concluded that it did not affect the sectional forces to a large extent. The reinforcement was meshed as layers. The reinforcement elements were sparsely meshed with elements having a size of 0.2 m x 10 m.

3.1.6 Application of load and load stepping

The load was applied using a loading sub-structure as mentioned in section 2.2. The sub-structure consisted of stiff beam elements that were connected to each other using tyings between the connected nodes. The purpose of the sub-structure was to distribute the load equally to all the 8 nodes on the surface of the slab. The load sub-structure is shown in Figure 10.

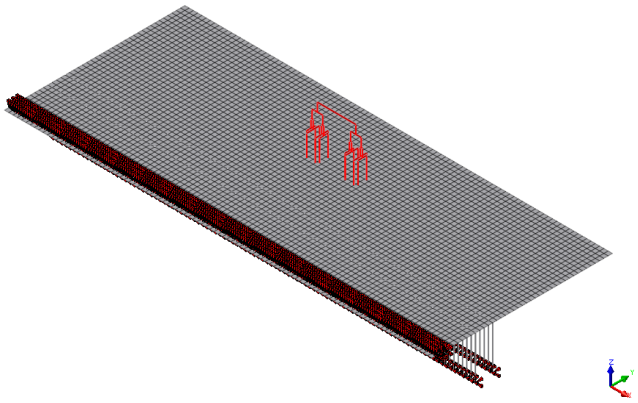

Figure 10 *FE-model of slab DR2-A showing the load sub-structure*

For linear analysis, the entire load was applied at once in the analysis. However, for non-linear analysis the load was applied in increments and an iterative procedure was used to find equilibrium for each increment.

Displacement control method was chosen for load application. Using displacement control, the analysis became more stable after formation of the cracks, which was

required in this project. In majority of the analysis, 10 steps for every 1mm of displacement of the load substructure were used.

3.1.7 Integration schemes

In the previous master theses by (Hakimi 2012) and (Kupryciuk, Georgiev, 2013), a 2x2 Gauss integration scheme was used in the plane of the quadrilateral element and 9 point Simpson integration scheme were used in the thickness direction. The above recommendations were used in all the analysis done in this master thesis.

3.1.8 Iteration method and convergence criteria

The iteration method governs the computing time required; therefore a suitable method needed to be selected. For all analysis, the BFGS iteration method with tangential convergence criteria with an accuracy of $10^{-3}$was used.

3.1.9 Choice of cracking model

The analysis in this project was done using the smeared crack approach. The crack bandwidth was chosen as 86mm based on the calculations from (Eurocode 2004)as shown in Appendix A.

3.2 Level I: Simplified Analysis

In level I analysis, one-way shear and punching shear resistances were calculated according to (Eurocode 2004)and the moment resistance was calculated using the yield line method and the moment resistance model in (Eurocode 2004). The results are shown below, for detailed calculations see Appendix A.

3.2.1 One-way shear resistance

One-way shear resistance was calculated at the critical section on the slab. The location of the critical section was determined according to the recommendations made in(BBK 2004).They are explained below.

The location of the critical section y_{cs} can, according to (BBK 2004)be calculated as:

$$y_{cs} = \frac{c + d}{2} \tag{1}$$

Where:

c = length of the area of load application
d = the average effective depth of the slab

The width of the critical section, b_w according to (BBK 2004) was calculated as the minimum of:

$$\begin{pmatrix} 7d + c + t \\ 10d + 1.3y_{cs} \end{pmatrix} \tag{2}$$

Figure 11 shows the location and width of the critical section on the slab used in this level of analysis.

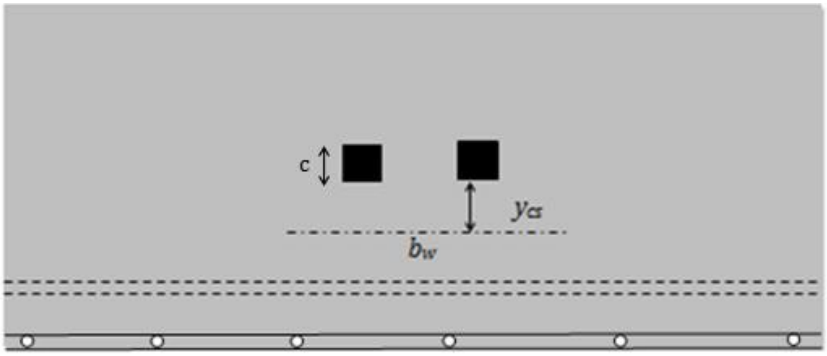

Figure 11 Location of the critical section, y_{cs}, and width of the critical section, b_w for calculation of one-way shear resistance.

The shear resistance of a concrete bridge deck without shear reinforcement $V_{Rd.c}$ was calculated using the recommendation in (Eurocode 2004) which is described below:

$$V_{Rd.c} = \left[C_{Rd.c}.k.(100\rho_1 f_{ck}).b_w.d\right] \quad (3)$$

Where:

$C_{Rd.c}$ = Co-efficient from tests

f_{ck} = Compressive strength of concrete

k = Co-efficient dependent on effective depth of slab

ρ_1 = Reinforcement ratio

d = Effective depth

b_w = Distribution width

The value for one-way shear resistance obtained at the critical section was 330kN. For level I analysis the value of applied load, was taken the same as the shear strength at the critical section.

3.2.2 Punching shear resistance

Punching shear resistance was calculated using the critcal section at a distance of $2d$ from the edge of the applied point loads, where d was the effective depth of the slab. The critical section for punching shear for slab DR2-A is shown in Figure 12. The perimter of the critical section b_0 was also evaluated.

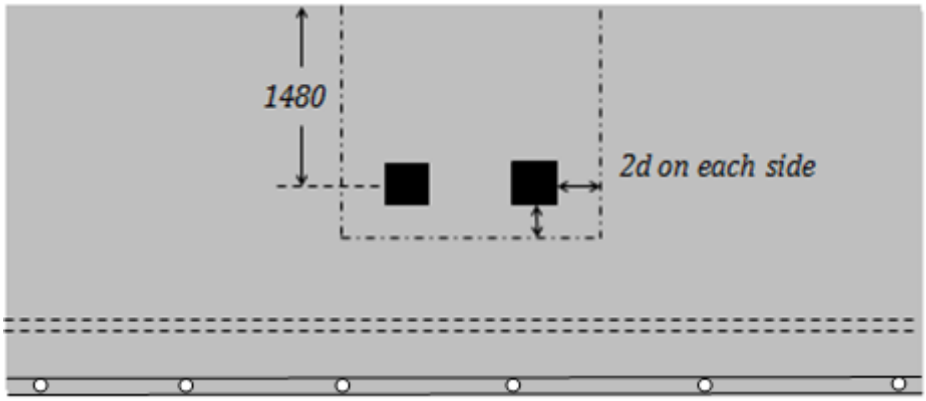

Figure 12 Area considered for evaluating punching shear strength.

According to (Eurocode 2004) the critical section for point loads should be at a distance of $2d$ from the face of the applied load, as shown in Figure 13. But since the punching shear capacity calculated according to critical section in Figure 12, was found to be more critical, that was the critical section that was used in this master thesis.

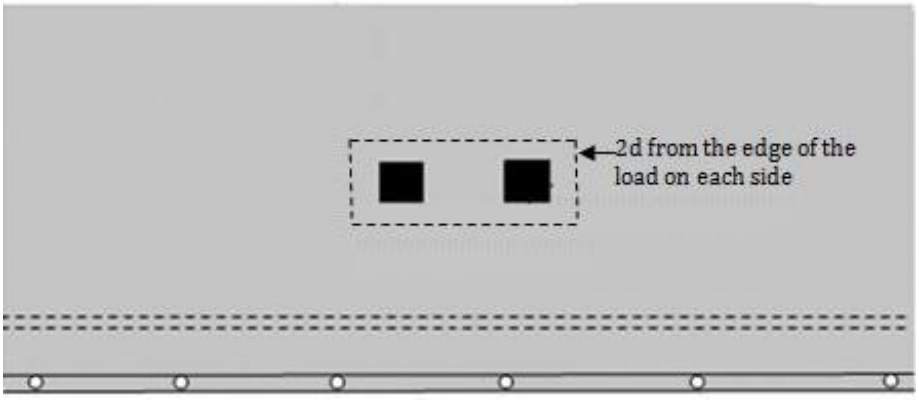

Figure 13 The recommendation in (Eurocode 2004)for critical section in punching shear

The punching shear resistance is calculated as follows:

$$v_{Rd.c} = C_{Rd.c}.k.(100\rho_1 f_{ck}) \quad (4)$$

Where:

$C_{Rd.c}$ = Co-efficient determined from tests

f_{ck} = Compressive strength of concrete

k = Co-efficient dependent on effective depth of slab

ρ_1 = Reinforcement ratio

To obtain the total punching capacity, $v_{Rd.c}$ was multiplied with the perimeter of critical section and the effective the depth of the slab. The force value obtained for punching shear capacity was 1149kN.

3.2.3 Flexural resistance

The moment resistance was calculated according to the yield line method. A yield line pattern that was kinematically feasible was selected (Hillerborg 1996). The yield line pattern used in this project is shown in Figure14.

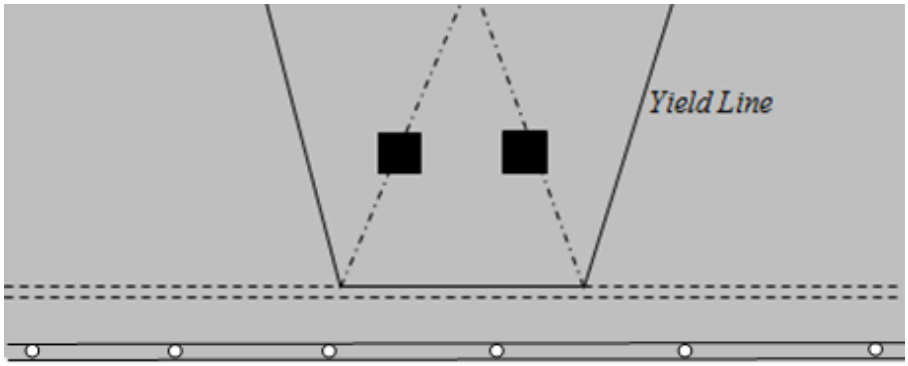

Figure 14 *Yield line pattern for the slab DR2-A. The solid lines show the yield lines at top while the dotted lines show the yield lines at the bottom of the slab.*

In accordance with the yield line pattern above, the energy conservation principle was applied to evaluate the flexural resistance. The equation used in calculations was as follows:

$$(Q * \delta) = (M * l * \theta) \quad (5)$$

Where:

Q = Applied load in a particular region
δ = Vertical displacement due to applied load
M = Moment resistance per meter of the yield line
l = Length of yield line
θ = Rotation of the yield line

Moment resistance was calculated to be1542 kNm. The maximum load in flexure as calculated by (Vaz Rodriguez 2007), was 1500 kN (Vaz Rodriguez 2007). The selection of the yield line pattern can be a possible reason for the difference in the values calculated in this project and the values calculated by(Vaz Rodriguez 2007), since the dimensions of the yield line pattern are selected by trial and error. See the Appendix A for detailed calculations.

3.2.4 Results and discussion

The load values corresponding to the three modes of failure are shown in Table 2. On the basis of these values it was concluded that the critical mode of failure was one-way shear. The results are summarized in Table 2.

Table 2 Simplified level of analysis, the maximum applied load that the slab can take for different modes of failure.

Mode of failure	One-way shear	Punching shear	Flexure
Applied load	330kN	1149kN	1542kN

Based on Level I analysis, it was concluded that the critical mode of failure of the slab was one-way shear since the punching shear and moment capacities were significantly higher. The redistribution of forces and moments due to non-linear response was only taken into account approximately and therefore the slab could e expected to take more load in reality than what was indicated by level I analysis.

The critical section for punching shear failure was assumed to extend all the way to the free edge as shown in figure 16. (Eurocode 2004) recommended a different critical section that was around the point of application of load. Calculations were done according to both the critical sections and the more critical one was chosen.

3.3 Level II: 3D Linear FE Analysis

For level II analysis the punching shear resistance was the same as in level I analysis. For one-way shear resistance a linear analysis of the slab was performed and the value of the applied load corresponding to the shear resistance in a critical section was evaluated. For performing the linear analysis, the FE model was first validated to ensure that the results were reliable. For flexural resistance, the results from the linear FE analysis and hand calculations were used.

3.3.1 Validation of the model

For the linear analysis of the slab to be credible the model needed to be validated first. The validation was done by checking two parameters:

- The deflection at free end after the application of self-weight was obtained through linear analysis and it was compared against the hand-calculated deflection of a simple cantilever beam.
- The equilibrium of all the vertical forces obtained through linear analysis was checked.

The deflection at the free end after the application of self-weight was found to be 0.544mm using linear FE analysis. The value obtained corresponds to the deflection calculated using a simple cantilever section, where the deflection at free end was found to be of 0.7 mm (see Appendix D). Linear FE-analysis result is shown in Figure 15.

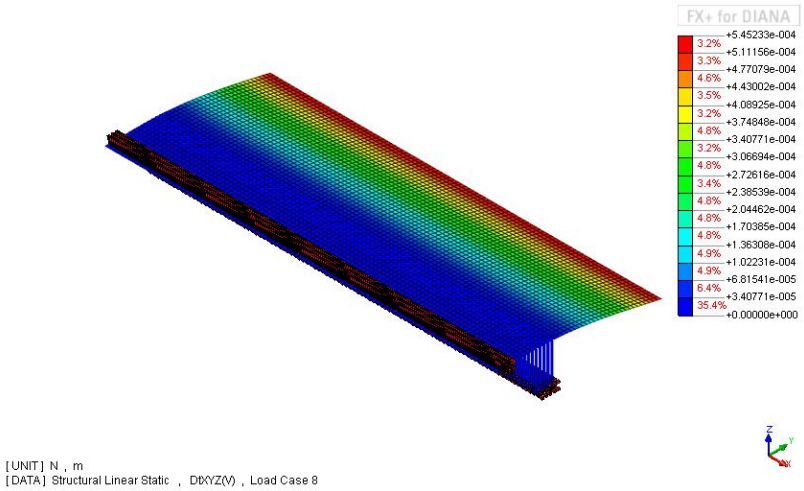

Figure 15 *Results from linear analysis of the slab DR2-A, showing deflections along z-axis.*

The equilibrium of vertical forces was checked using the reaction forces from the linear FE analysis. The sum of the vertical reaction forces at the supports was equivalent to the applied external loading and thus the structure was in equilibrium. Both validation parameters were fulfilled in the linear analysis.

3.3.2 One-way shear resistance

As the shear force is transferred towards the support it gets distributed over a certain distribution width as explained in section 3.2.1. Owing to this distribution, the one-way shear resistance at a critical section and the corresponding value of applied load were not expected to be the same in level II analysis. The value of the applied load was expected to be greater than that at the critical section since a part of the total applied load would be transferred to the supports without passing the critical section.

To obtain the value of the applied load a linear analysis was conducted and the corresponding value of 884kN was obtained that showed the applied load. This value was higher than the applied load value for level I analysis (330 kN). The distribution of shear forces across the slab is shown in Figure 16.

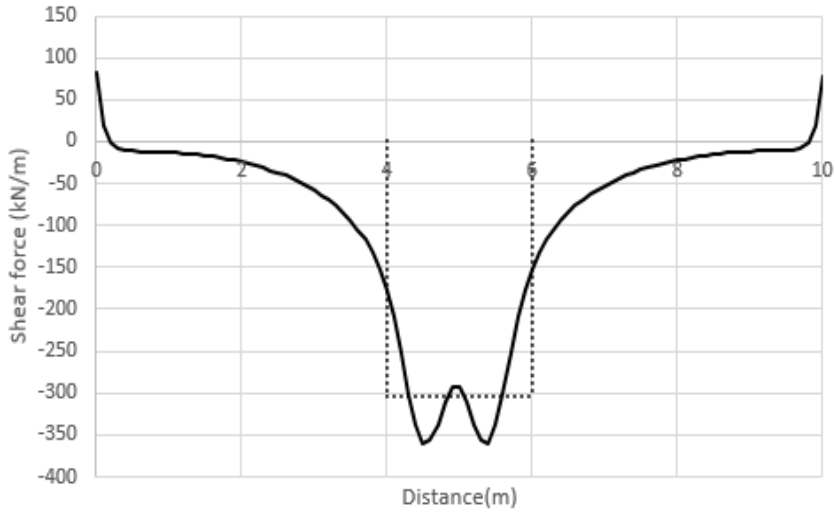

Figure 16 *Shear force distribution in transversal direction according to linear analysis. Dotted line shows the distribution width.*

To calculate the the critical value in one-way shear, an average of the shear force values was obtained over the distribution width at the critical section of the slab. The dotted line in Figure 17 shows the average value of shear force at the critical section, and also the distribution width over which the average was calculated. This average value was then used to extract the value of applied load from linear FE analysis. The vaue of applied load was found to be 884kN.

3.3.3 Punching shear resistance

For level II assessment the punching shear resistance was calculated using (Eurocode 2004), and therefore the resistance remained the same as for level I assessment.

3.3.4 Flexural resistance

For level II assessment, the flexural resistance was calculated by performing linear FE analysis of the slab and the recommendations in(Pacoste *et al* 2012) were used. According to(Pacoste *et al* 2012) the distribution width for moment distribution could be calculated as:

$$w_x = 2d + b + t \tag{6}$$

Where:

w_x = distribution width
d =effective depth of the slab
b = width of the area of load application
t = thickness of the top layer

The location of the critical section, y_{cs} for flexural failure was taken at the spring support in the FE model. The location and width of critical section are shown in the Figure 17.

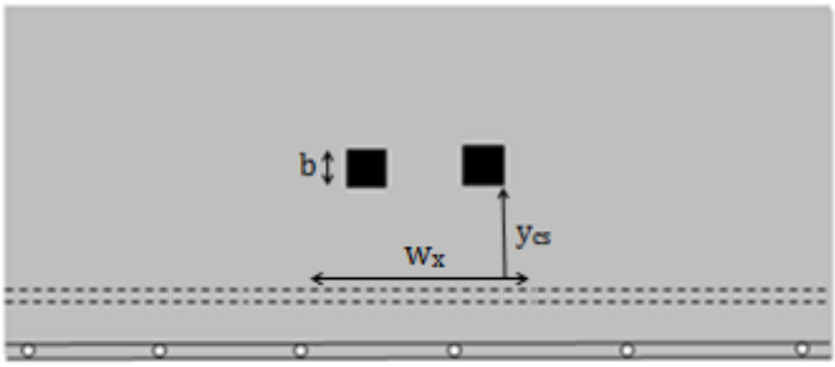

Figure 17 Location and width of the critical section in flexural failure as recommended in (Pacoste et al 2012).

A linear FE analysis of the slab was performed. The moment values across the width of the critical section w_x were obtained from the linear analysis. An average moment value was then obtained.

This average value was compared against the capacity of a unit width of slab that had been obtained through hand calculations. When these two values were similar the

corresponding applied load was extracted from the linear analysis and that was the flexural capacity of the slab. It was found to be 1250kN.

3.3.5 Results and discussion

The load values corresponding to the three modes of failure are shown in Table 3.

Table 3 Results from level II analysis of the slab.

Mode of failure	One-way shear resistance	Punching resistance	Flexural resistance
Applied load	884kN	1108kN	1250kN

From the values in Table 3, it was concluded that the mode of failure was one-way shear failure. Since the re-distribution of shear force was taken into account for this level of assessment, the slab showed a higher resistance in one-way shear than level I.

The failure load in level II of structural analysis using 3D linear FE model was evaluated to be 884 kN. The value was on the conservative side compared and was 8% less than the failure load of 961 kN as obtained from the experiments conducted by (Vaz Rodriguez 2007).

This could be attributed to the fact that reinforced concrete had a typical non-linear response which cannot be accurately depicted in linear FE model. For example, linear analysis did not account for plastic redistribution of sectional forces due to the yielding of reinforcements, which increased its load carrying resistance to some extent. This phenomenon was later investigated in this project and is explained in the later sections.

3.4 Level III: non-linear analysis

Level III analysis provided resistance values for reinforced concrete after the redistribution had been taken into account. The one-way shear and punching shear resistance were calculated according to the recommendations in Model Code 2010 (CEB-FIP, 2013). A non-linear analysis of the slab was performed to obtain the sectional forces after redistribution had occurred. For the non-linear analysis to be reliable the model was first validated by comparing the results from the non-linear analysis with the results from (Vaz Rodriguez 2007).

3.4.1 Validation of the model

Figure 18 shows the FE-model for slab DR2-A.

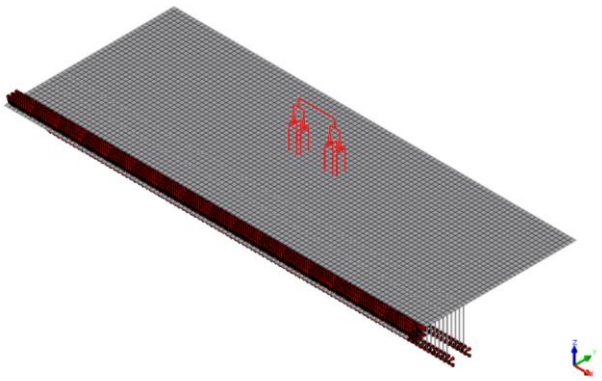

Figure 18 FE-model of slab DR2-A used in this project.

To validate the model the load deflection curve from the non-linear analysis was obtained and was compared against the load deflection curves from both the non-linear analysis and the experiment performed in (Vaz Rodriguez 2007). The curves are shown in Figure 19.

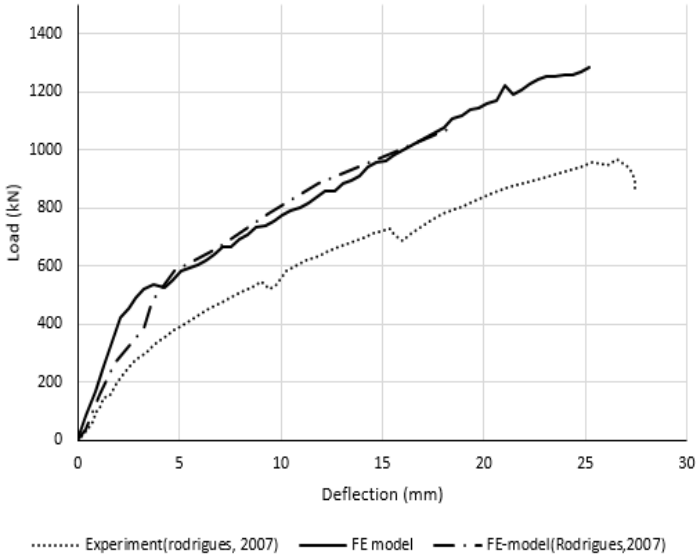

Figure 19 Load deflection curve from this project compared with that from FE-model of (Vaz Rodriguez 2007)and (Vaz Rodriguez 2007)experiment. Apart from the curve with solid line, the other two curves were adopted from (Vaz Rodriguez 2007).

Results from non-linear analysis done in this project showed a significantly stiffer behavior than the results from the experiment(Vaz Rodriguez 2007). The higher stiffness in the linear part of the load deflection curve could be explained by the pre-loading condition, which was explained in section 2.2.1. Because of the pre-loading, the slab had possibly cracked before the failure load was applied and therefore in the experiment the slab showed a less stiff behavior in linear phase. However, the difference in stiffness in the non-linear part of the curves was still not explained by the preloading condition. Possible reasons for the deviation from the experimental results were investigated in the later sections.

The load deflection curve for slab DR2-A from this project was also compared with the load deflection curve from the FE model in (Vaz Rodriguez 2007) as previously shown in Figure 20.

It was seen that the load deflection curve, in the FE model in (Vaz Rodriguez 2007) and that in this project were very similar. So it could be possible that there were some conditions during the experiment that influenced the stiffness of the slab but were not accounted for in the FE-model. But there was not enough information or evidence in (Vaz Rodriguez 2007) to decide what exactly was the reason for this difference in stiffness between the FE-model and experiment.

Since the modeling choices made by (Vaz Rodriguez 2007)were not known, the model in this project still could not be validated only on the basis of the similarity between the load deflection curves from the two FE-models. Further verification was still needed for the model in this project to be reliable.

For further verification, the same FE-model was used but the loading condition and reinforcement ratio were changed. First they were changed to match specifications of slab DR1-A and then changed to match specifications of slab DR2-C from (Vaz Rodriguez 2007). For detailed description of the specifications of slab DR1-A and DR2-C see section 2.1. All other modeling choices were kept the same as that for the FE-model of slab DR2-A. The non-linear analysis for DR1-A and DR2-C was performed and results compared against the experimental results for these two slabs from (Vaz Rodriguez 2007), to see if the model can be validated.

DR1-A: 4 point loads

A 4-point load scenario was considered on slab DR1-A. The FE-model for this slab is shown in Figure 20. The reinforcement ratio in this particular slab was 0.79% and the model was modified accordingly before a non-linear analysis was performed.

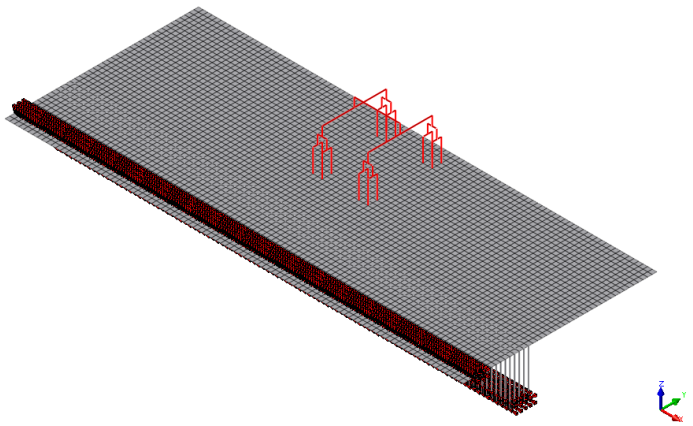

Figure 20 Slab DR1-A was subjected to four point loads.

The load deflection curves from the FE-model and experiment for slab DR1-A are shown in Figure 21. The FE-model showed stiffer behavior in the linear phase, but that could be explained because of the fact that in the experiment slab DR1-A was pre-loaded and thus possibly cracked before failure load was applied. This could have led to a less stiff response in linear phase during the experiment. The behavior in the non-linear phase was similar. The FE-model was therefore seen to behave in an acceptable manner.

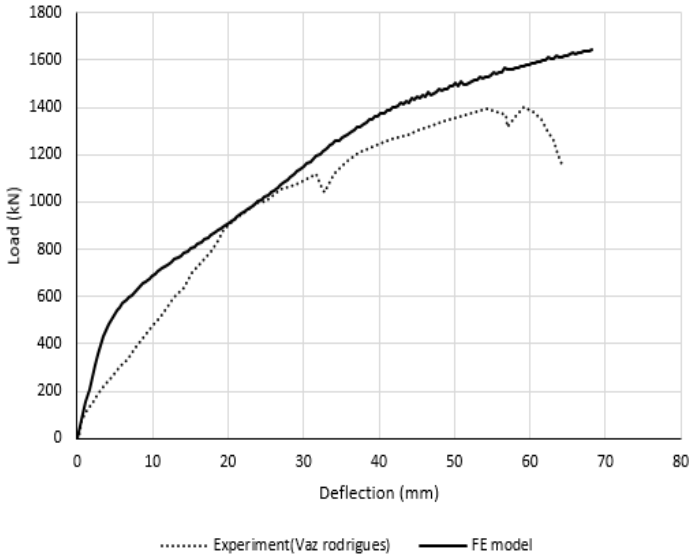

Figure 21 *Load deflection curves for slab DR1-A. It shows comparison of the curve obtained from non-linear analysis with the curve obtained from the experiment.*

DR2-C: Single point load at the edge

To further investigate the stiff behavior of the slab DR2-A, another load case from (Vaz Rodriguez 2007) with a single point load on DR2 slab was modeled and analyzed. In this load case, the influence of edge reinforcement was taken into account by modeling an edge beam on the sides of the bridge deck. Figure 22 shows the test case as well as the FE-model.

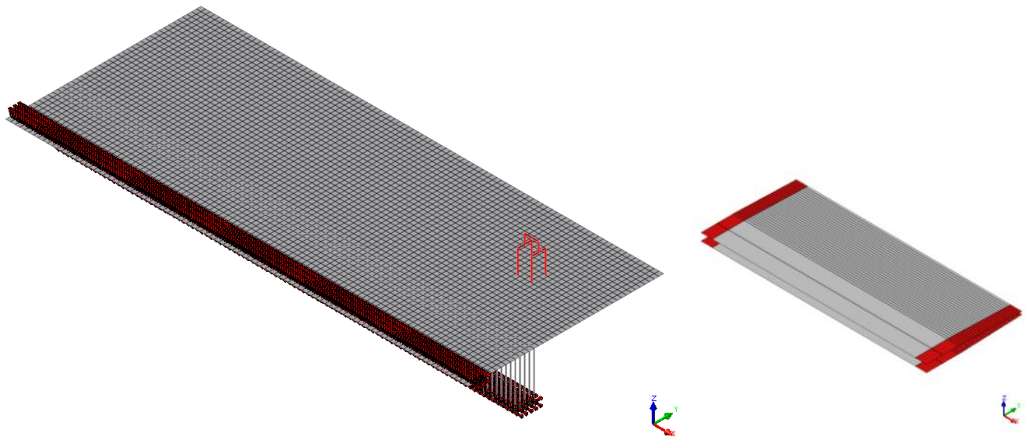

Figure 22 *FE-model of slab DR2-C used in the experiment and the reinforcement model.*

A non-linear FE analysis was performed and the load versus deflection curve was plotted against the experimental results. The curves can be seen in Figure 24.

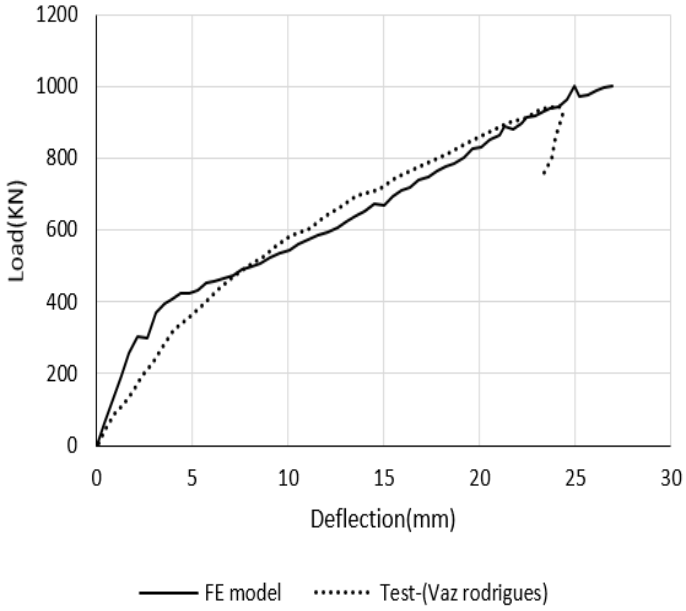

Figure 23 Load vs Defelction curve for slab DR2-C and from(Vaz Rodriguez 2007)experimen. The dotted curve is adapted from (Vaz Rodriguez 2007).

Figure 23 shows that the results from the FE-model and the experiment show considerable agreement as the stiffness in non-linear phase is similar. The model in case of slab DR2-C was thus seen to behave in an acceptable manner.

Based on the above investigations, the modeling choices used for slab DR2-A were judged to be valid. The stiff behavior during linear phase of the original case (DR2-A), could be attributed to the pre-loading done on the slab in the actual experiment. Based on the other two analysis this FE- model was deemed reliable for further study and there was enough evidence to continue using the model in this project.

3.4.2 One-way shear Resistance

Model Code 2010 (CEB-FIP, 2013)was used to evaluate one-way shear resistance of the slab for level III analysis. The value for one-way shear resistance was evaluated according to the equation below:

$$V_{Rd.c} = k_v \frac{\sqrt{f_{ck}}}{\gamma_c}.z.b_w \quad (7)$$

Where:

z = Centre to centre distance between top and bottom reinforcement

b_w = Distribution width

γ_c = Partial safety factor for concrete

k_v =Co-efficient dependent on effective depth of slab

f_{ck} = Compressive strength of concrete

For this level of analysis the value for k_v was evaluated according to the equation below:

$$k_v = \frac{180}{1000 + 1.25z} \tag{8}$$

The distance of the critical section from the support was taken as equivalent to the effective depth d of the slab. Since the slab is tapered and the depth is not constant, the effective depth d was chosen as the depth at the thickest end of the slab as recommended in Model Code 2010 (CEB-FIP 2013), see Figure 24.

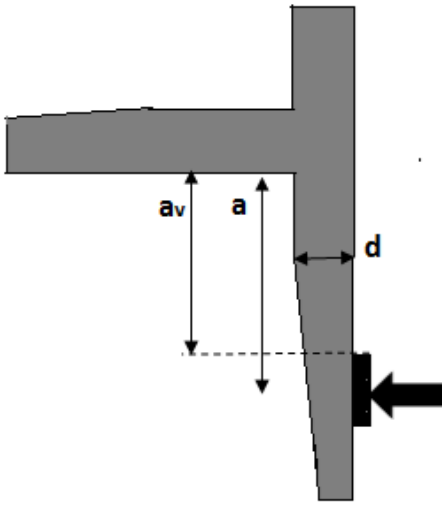

Figure 24 *Recommendation in Model Code 2010 (CEB-FIP 2013) for selection of distribution width b_w, figure is adopted from Model Code 2010 (CEB-FIP 2013). The figure shows a cantilever slab with load applied near the free end.*

The value for the distribution width b_w was chosen for the case when the slab has clamped supports. The distribution width formed an angle of 45 degrees with the point of application of the load. The recommendation in Model Code 2010 (CEB-FIP, 2013)for selecting b_w and d is shown in Figure 25.

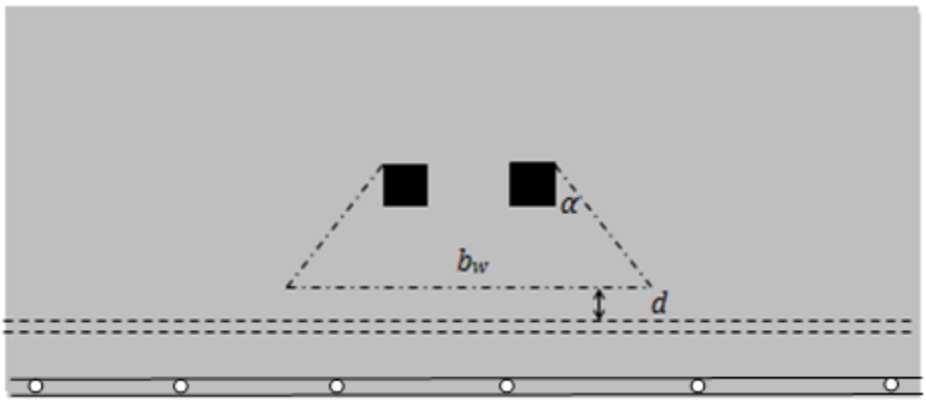

Figure 25 *The location of the critical section and the distribution width that is used in this project. The critical section is indicated by the dotted line and a value of 45^o is chosen for the angle α.*

There was no recommendation in Model Code 2010 (CEB-FIP 2013) for the case where two point loads were applied close to one another. It was assumed that if distribution width corresponding to each point load was added it would give a final distribution width for two point loads. Due to this choice there was a risk that the

value of distribution width (b_w) would be over-estimated, but it was seen as the most acceptable way to proceed with the calculations given that no better alternate was available. The value of that was used in calculations for this project is shown in Figure 26.

The value of one-way shear resistance at the given critical section was evaluated as 321kN. This value was then used in the non-linear analysis to evaluate the corresponding value for the applied load. The value of applied load was1171kN.

Proposed method for calculating the distribution width

Model Code 2010 (CEB-FIP 2013)did not have any recommendation to calculate distribution width in case two point loads act close to one another. The same method as in the case of a single point load was therefore followed to calculate the distribution width for this project. However, this lead to an over estimation of the distribution width, which also caused an over estimation in the value of one-way shear resistance. The value for one-way shear resistance according to (Vaz Rodriguez 2007) was 961 kN, but the value obtained through the non-linear analysis done in this project was found to be 1171 kN, which is significantly higher.

To counter this problem, an improved method for calculating the distribution width was suggested in this project. The transversal shear force distribution at the failure load of 1171kN was obtained from non-linear analysis. Then a linear trend-line was drawn through the distribution. When this linear trend-line became horizontal it showed that the shear force across that distance was more or less constant. This distance was then used as the distribution width and a new value for the one-way shear resistance was calculated using Equation 7.

Figure 26illustrates the procedure for selecting the improved distribution width.

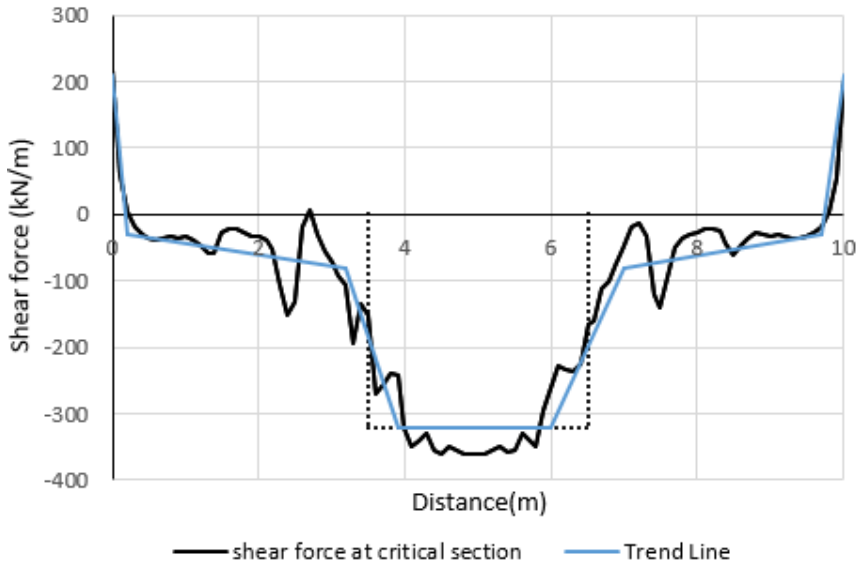

Figure 26 Shear force distribution in slab DR2-A.

Figure 26, shows the longitudinal shear stress distribution at the applied load of 1171kN. The dotted line shows the distribution width according to Model code 2010 (CEB-FIP 2013)recommendations which has a value of 3.1m. The horizontal part of the trend-line shows the distribution width according to the proposed method which has a value of 2.2m.

According to the improved distribution width the one-way shear resistance at the critical section was obtained as 228kN and the corresponding value of the applied

load V_E from non-linear analysis was obtained as 940kN. The transversal shear force distribution at the new one way shear resistance value of 940kN is shown in Figure 27.

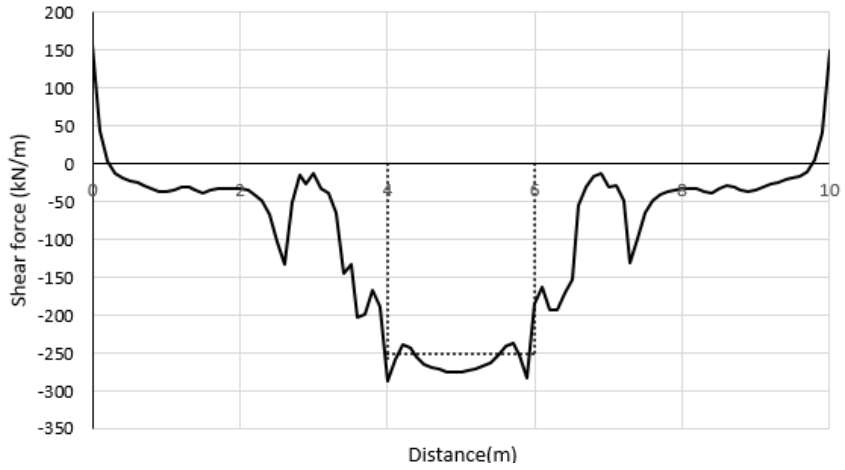

Figure 27 Shear force distribution at the new failure load of 940kN, which was determined according to the new proposed method.

On the basis of this new proposed method for calculating distribution width, the one-way shear resistance value was closer to the failure load value of 961 kN in (Vaz Rodriguez 2007) and thus depicted the actual load carrying capacity of the slab better.

3.4.3 Punching shear resistance

For level III analysis, the punching shear resistance was evaluated by the application of critical shear crack theory (CSCT) by Muttoni according to Model Code 2010(CEB-FIP 2013). According to this method the punching shear strength V_R is dependent on the rotation ψ of the slab. The value of rotation ψ was calculated as the difference in rotation at point a_1 and a_2 as shown in Figure29. The perimeter of the critical section is evaluated at a distance of $0 \cdot 5d$ from the edge of the loaded area.

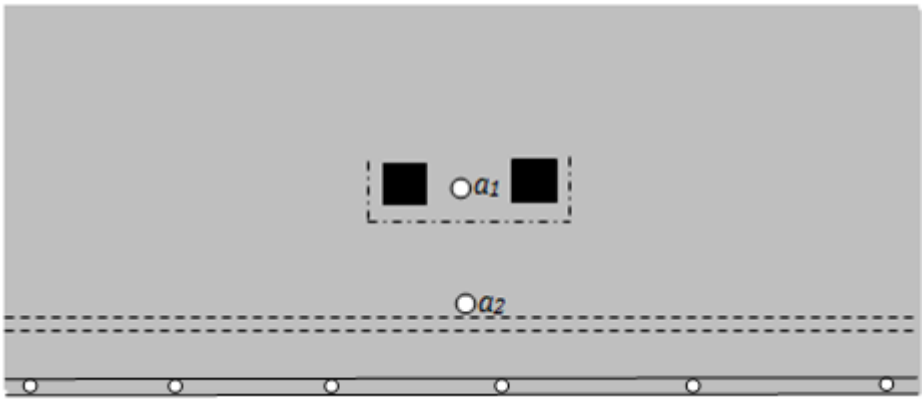

Figure 29 Recommendation in Model code 2010(CEB-FIP 2013) for the critical section in case of punching shear.

The failure criterion used to evaluate the punching shear resistance is shown below.

$$\frac{V_R}{b_0.d\sqrt{f_{ck}}} = \frac{3/4}{1+15\psi\frac{d}{d_{g0}+d_g}} \quad (9)$$

Where:

d = Average effective depth of slab

b_0 = Distribution width

d_{g0} = Reference aggregate size

d_g = Maximum aggregate size

f_{ck} = Compressive strength of concrete

ψ = Rotation of the slab evaluated as the difference in rotation at points a_1 and a_2

The applied load versus rotation curve was obtained from non-linear analysis and super imposed over the curve obtained from the failure criteria suggested in (Muttoni 2009) and shown in Equation 9. The point where these two curves intersected was equivalent to the failure criteria presented in Equation 9. The curves are shown in Figure 30.

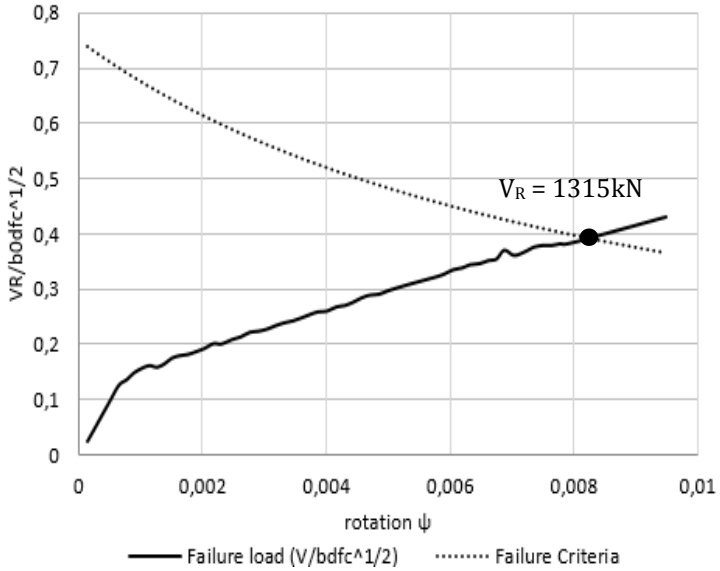

Figure 30 Evaluation of punching shear resistance for slab DR2-A.

The value at the point of intersection was used to evaluate a value for V_R by using the failure criteria in Equation9. The value obtained was 1315 kN.

3.4.4 Flexural resistance

In level III, the flexural resistance was calculated on the basis of rupture of reinforcement bars. The reinforcement bars were tested in tension (Vaz Rodriguez 2007) and it was found that the top reinforcement for the test specimen, DR2 had a tensile failure strain of 14%(Vaz Rodriguez 2007).The strain value was extracted from the non-linear analysis and the corresponding load for which rupture of reinforcement takes place was found to be 1898 kN. Thus the flexural resistance according to non-linear analysis was 1898 kN.

3.4.5 Results and discussion

The results from non-linear analysis are summarized in Table 4.

Table 4 Summary of results from level III analysis.

Mode of failure	One-way shear resistance	Punching resistance	Flexural resistance
Applied load	1171kN (MC recommendation) 940kN (proposed method)	1315kN	1898kN

Based on the results, it was seen that mode of failure was one-way shear. This correspondedwell with the results from (Vaz Rodriguez 2007).The load deflection curve of slab DR2-A showed stiffer response than the experiment. But based on the results from non-linear analysis of slabs DR1-A and DR2-C the modeling choices were verified and were seen to be acceptable. Also the shear force and moment distribution obtained for slab DR2-A were in accordance with how the slab was expected to behave. The exact reason for why slab DR2-A showed a stiffer response than the experiment (Vaz Rodriguez 2007) remains to be determined.

3.5 Conclusion

Figure 31summarizes the results from all three levels of structural assessment and depicts the difference in failure load of slab DR2-A at each level of structural assessment.

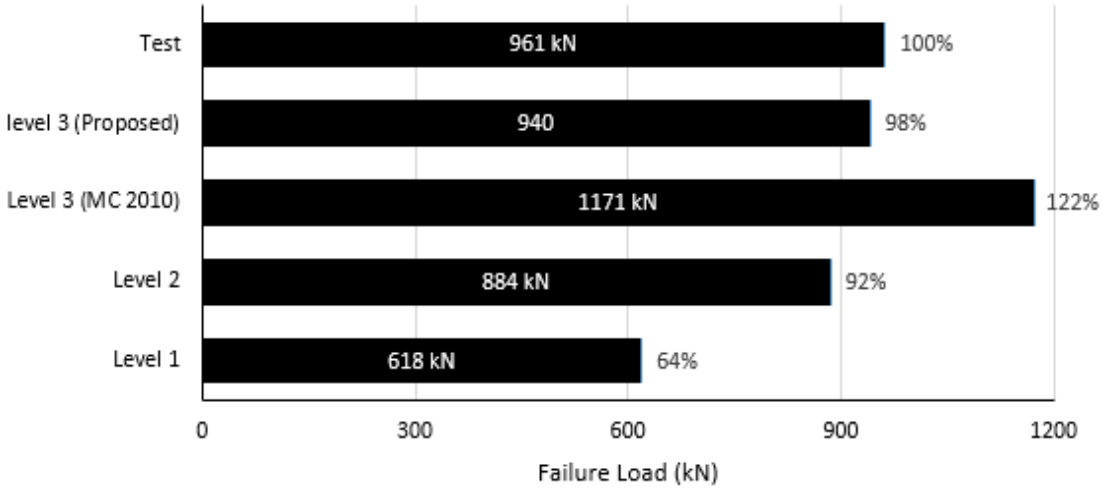

Figure 31 Conclusion from the multi-level structural assessment of slab DR2-A.

Level I structural assessment did not take in to account redistribution of shear forces and moments and therefore showed lesser failure load than other two levels of assessment. In reality re-distribution of forces and moments occurs after cracking and the structure has the ability to take more load than what level I assessment would suggest.

Level II structural assessment used linear FE analysis to compute sectional forces and the results depicted the behavior of the structure more accurately than level I assessment. However after cracking occurred and the structure started to behave non-linearly, it could still have taken more load because the loads get distributed to the stiffer parts of the structure. Therefore linear analysis still under-estimated the failure load of the structure.

Level III of structural analysis used Model Code 2010(CEB-FIP 2013)to evaluate resistance of the structure in punching and one-way shear and also used 3D non-linear FE analysis to compute the sectional forces in the slab. Non-linear analysis took the redistribution of forces after cracking into account and therefore was seen to give a failure load that was closer to the one in reality.

The failure load obtained from non-linear FE analysis was overestimated by 22% as compared to failure load in (Vaz Rodriguez 2007). The mode of failure in the experiment and in the non-linear FE analysis was one-way shear. But, the failure load from non-linear analysis was higher and a possible reason could be the over-estimation of distribution width b_w. The distribution width was calculated according to recommendations inModel Code 2010 (CEB-FIP, 2013), but the code has no specific provision for the case when two point loads are applied close to one another. Since one-way shear resistance was significantly dependent on the distribution width, the failure load from non-linear analysis came out to be higher than the experiment.

For a more accurate calculation of the distribution width a new method was proposed in this project. The proposed method gave a distribution width of 2m and one-way shear resistance of 940kN. This resistance value is closer to the actual failure load

value obtained in (Vaz Rodriguez 2007) and therefore it can be concluded that the proposed method did give better results in this particular case.

However, the method was only a hypothesis at this stage and needs further verification and analysis before it could be seen as a reliable way of calculating the distribution width.

In level III analysis of slab DR2-A, the load deflection curve was stiffer than the results from the experiment. Although the modeling choices made in this project were validated by comparisons with slab DR1-A and DR2-C but the reason for the stiff response for slab DR2-A remains to be verified.

The value for flexural resistance obtained is notably high; it proved to be non-critical in the evaluation of the failure load. Therefore the moment re-distribution could not be studied in case of slab DR2-A.

4 Parametric Studies

To investigate the influence of certain parameters on the structural response of the bridge cantilever slab, parametric studies were performed. A multi-level structural assessment was performed for each parametric variation. Table 5summarizes the parametric variations. The blue color in the table indicates the reference model.

Table 5 Summary of parametric studies, the blue parts indicate the reference models.

Parametric Study		
Geometrical Variations	Influence of edge beams	No edge beam.
		Edge beam at free end.
	Span/depth ratio	Span and depth of the slab as in (Vaz Rodriguez 2007)
		Span kept constant, depth of the slab doubled.
	Reinforcement Ratio	Intermediate (0.6%)
		High (2.1%).
Stiffness	Support stiffness	Springs have no stiffness in tension and high stiffness in compression.
		Spring stiffness in compression reduce to $1/10^{th}$

4.1 Influence of support stiffness

To depict the box girder that supports a bridge deck slab, springs were used in the FE-model. Stiffness of the springs showed the influence of stiffness of the box girder on the structural response of cantilever bridge deck slab. In this parametric study, stiffness of the non-linear springs in compression, was reduced to a 10^{th} of their value. The stiffness in tension was maintained as zero. All other modeling choices, parameters and boundary conditions were kept the same as the original model.

4.1.1 Level I analysis

The resistance values in level I analysis were the same as that in the reference model. They are summarized in Table 6:

Table 6 Level I analysis for slab with reduced spring stiffness.

Mode of failure	One-way shear	Punching shear	Flexure
Applied load	330kN	1108kN	1542kN

4.1.2 Level II analysis

In level II analysis, the punching resistance values were same as that in level I. The applied load value for one-way shear resistance changed because at this level shear force re-distribution was taken into account. This value was extracted from the linear

analysis of the model and was 940kN. The flexural resistance value was evaluated using the same method as in section 3.3.4 and was found to be 1592kN.

The results from level II analysis are summarized in Table 7.

Table 7 Level II analysis for the model with reduced spring stiffness.

Mode of failure	One-way shear	Punching shear	Flexure
Applied load	920kN	1108kN	1592kN

4.1.3 Level III analysis

A non-linear analysis was performed and a load versus deflection curve is shown in Figure 32. The load deflection curve for the reference model is also shown in the same figure for comparison.

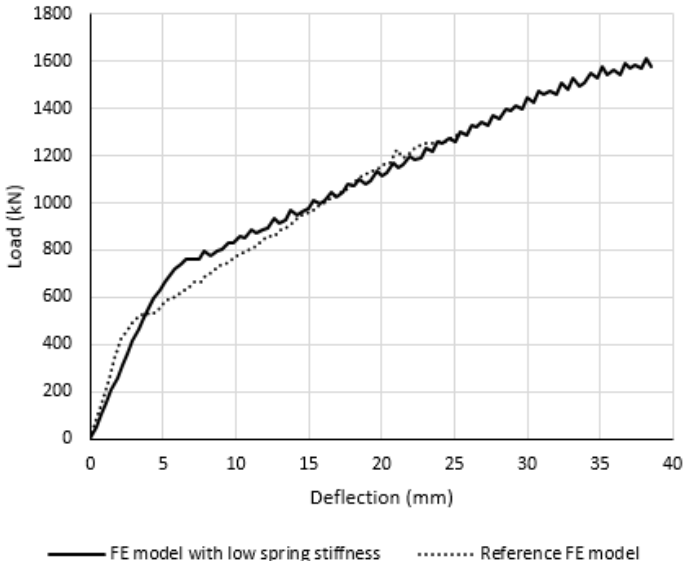

Figure 32 Load deflection curve for the reference model and the model with reduced spring stiffness.

As shown in the figure, the model with reduced stiffness of springs showed a less stiff response in the linear phase than the reference model. The behavior in the non-linear phase however was similar for both the models. Also, the cracking occurred at a higher load with lower spring stiffness than the reference model.

4.1.3.1 One-way shear resistance

The one-way shear resistance remained the same as in the reference model as there was no provision in Model Code 2010 (CEB-FIP, 2013) to account for the stiffness of the supports. Thus the location and width of the critical section remained the same as in the reference model. One-way shear resistance at the critical section had a value of 321kN and the corresponding failure load was evaluated to be 1303 kN.

The new proposed method for evaluating the distribution width was also tested for this parametric study. The longitudinal shear force distribution at the one-way shear resistance value of 1303kN was obtained and a trend line was drawn. It is shown in Figure 33.

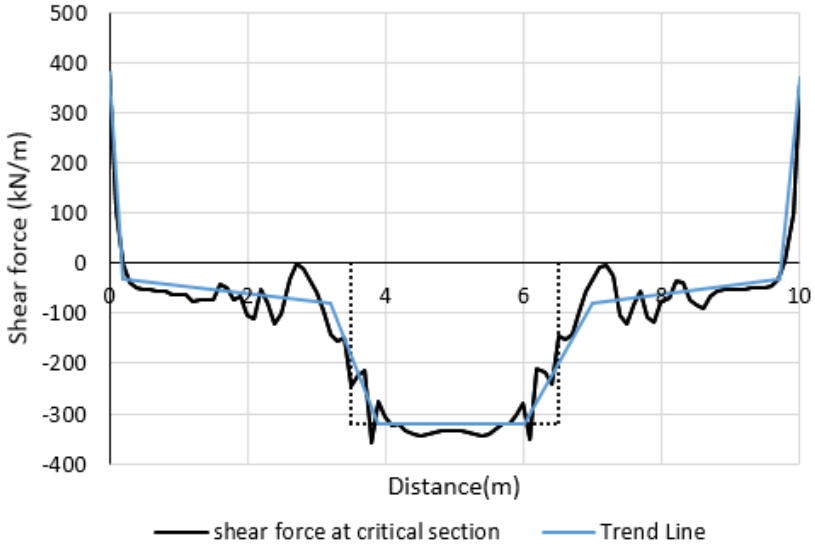

Figure 33 *Shear force distribution along the section in the model with lower spring stiffness.*

The distance over which the trend-line is horizontal was taken as the new distribution width. The new distribution width was 2.1m and the new one-way shear resistance at the critical section was 218kN. According to this value at the critical section, the applied load value came out to be 1070kN.

4.1.3.2 Punching shear resistance

Punching shear resistance was calculated based on critical shear crack theory (CSCT) by Muttoni according to Model Code 2010 (CEB-FIP, 2013). Since the model with low spring stiffness had similar rotation values as the reference model (as seen in Figure 32), there was no significant change in the punching shear resistance. The failure load with respect to punching was 1315kN, same as that of the reference model. Figure 34 shows the failure load and the failure criteria curves that were used to evaluate the punching shear capacity.

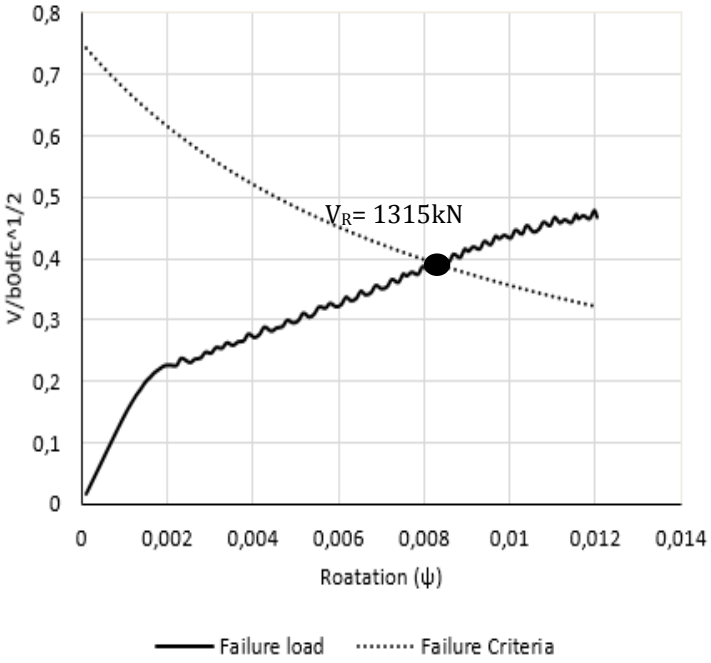

Figure 34 Evaluation of the punching shear resistance of the slab using CSCT.

4.1.3.3 Flexural resistance

The flexural resistance was calculated using the same method as in the case of the reference model.From the strain values obtained from non-linear analysis, it was found that the rupture of the reinforcement occurred at a load of 2320 kN. So the flexural resistance was 2320 kN.

4.1.4 Results and discussion

The results from the analysis of the model with low spring stiffness are shown in Table 8.

Table 8 Summary of the results from non-linear analysis of the model with lower spring stiffness.

Mode of failure	One-way shear resistance	Punching resistance	Flexural resistance
Applied load	1320kN (MC recommendation) 1047kN (proposed method)	1315kN	2320kN

If the distribution width used was according to Model Code 2010 (CEB-FIP, 2013), the mode of failure in level III was found to be punching shear failure and the failure load was 1315kN. When the new proposed method for calculating distribution width was used then the mode of failure in level III analysis was found to be one-way shear and the failure load was 1047kN. Figure 35 shows the failure load value for each level of analysis and compares them with the reference model failure load values.

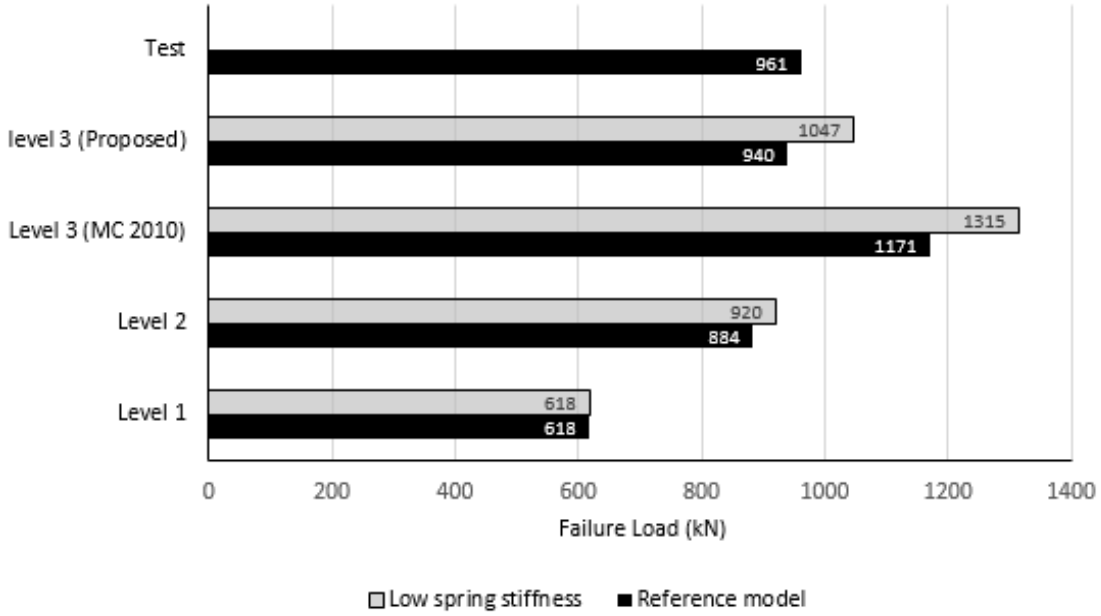

Figure 35 *Comparison of the model with lower spring stiffness with the reference model.*

From the non-linear analysis of the slab an interesting observation was that a greater amount of shear force got transferred to the clamped support. It is shown in Figure 36.

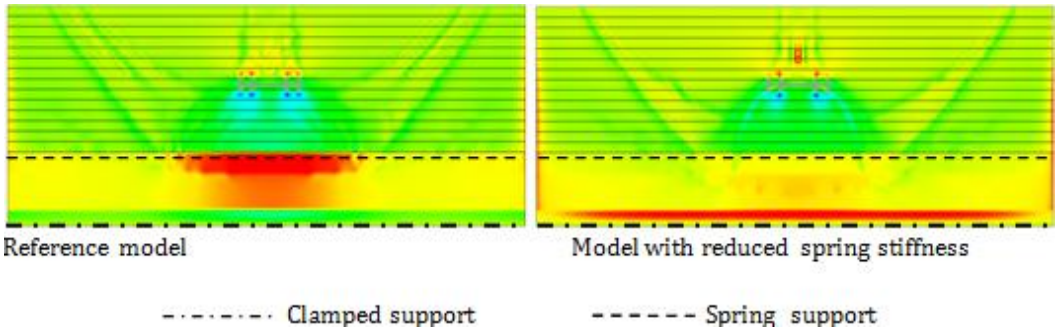

Figure 36 *The difference in shear force distribution between the reference model and the model with lower spring stiffness.*

But since the region of shear failure was between the support and the load, this change in the distribution of shear forces between the two supports did not concern the scope of this project. The region of interest was the part between the load and the support and the distribution there was to be analyzed.

Figure 37 shows the transversal distribution of shear forces before and after the reduction in spring stiffness.

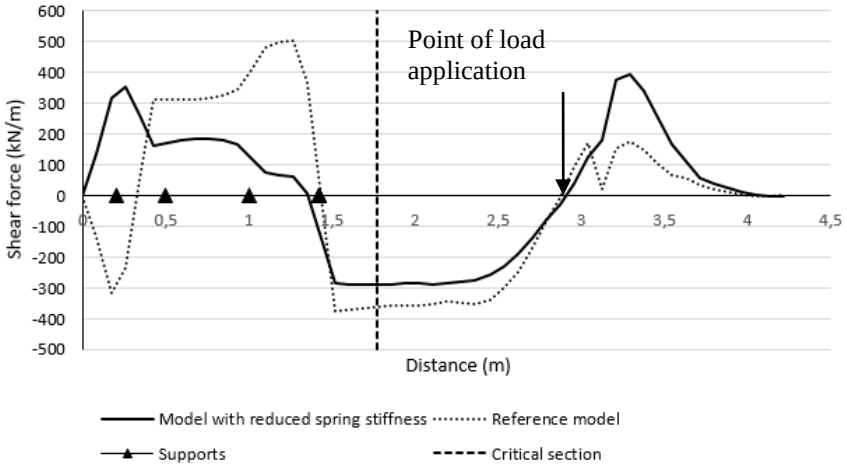

Figure 37 Difference in longitudinal distribution of shear forces between the reference model and model with reduced spring stiffness

In Figure 37 it can be seen that in the part between the support and the load, the amount of shear force had reduced as compared to the reference model. This allowed the applied load value to be higher in case of reduced spring stiffness and this explained why a higher one-way shear failure load was obtained in this model as compared to the reference model.

It was observed that the one-way shear resistance was higher according Model Code 2010 (CEB-FIP, 2013) recommendations and also according to the new proposed method of calculating distirbution width. Table 9 shows the comparison of the one-way shear resistance values for the reference model and the model with reduced spring striffness.

Table 9 Comparison of one-way shear resistance in reference model and model with reduced spring stiffness.

Model	One-way shear resistance Model code 2010	One-way shear resistance Proposed method
Reference model	1171kN	940kN
Reduced spring stiffness	1352kN	1047kN

It was concluded on the basis of this analysis that the one-way shear resistance increased with decreased support stiffness.

The punching shear resistance for this model was the same as that of the reference model. This could be explained using critical shear crack theory. According to CSCT, punching shear resistance is a function of rotation of the slab. In the linear phase, the model with reduced stiffness showed higher rotation. After cracking occurred, the influence of support stiffness had no affect the rotation of the slab. This explains why there were similar rotation values for the reference model and the model with reduced stiffness. This ends up reflecting in the punching shear resistance value as well, which was same for both the models.

4.2 Span to depth ratio

To study the influence of span depth ratio on the structural behavior of bridge deck slab, the depth of the entire slab was doubled, while all other parameters and modeling choices were kept the same. A multi-level structural assessment was then performed.

4.2.1 Level I analysis

In level I analysis the one-way and punching shear resistance was obtained according to (Eurocode 2004). See section 3.2.1 and 3.2.2 respectively for details about the method of evaluation. For detailed calculations see Appendix B. The results are summarized in Table 10.

Table10 Summary of results from level I analysis of slab with twice the depth

Mode of failure	One-way shear	Punching shear	Flexure
Applied load	1000kN	2718kN	3134kN

4.2.2 Level II analysis

In level II analysis, the punching resistance values were same as that in level I. The failure load for one-way shear resistance changed owing to the linear distribution of sectional forces. The value of the failure load was extracted from the linear analysis of the model and was 4500kN. The flexural resistance value was evaluated according to the method outlined in section 3.3.4 and was found out to be 3500kN.The results from level II analysis are summarized in Table 11.

Table 11 Summary of results from level II analysis of slab with twice the depth

Mode of failure	One-way shear	Punching shear	Flexure
Applied load	4500kN	2718kN	3500kN

4.2.3 Level III analysis

A non-linear analysis was performed with the span kept constant and the depth of the slab doubled. Figure 38 shows the load deflection curve.

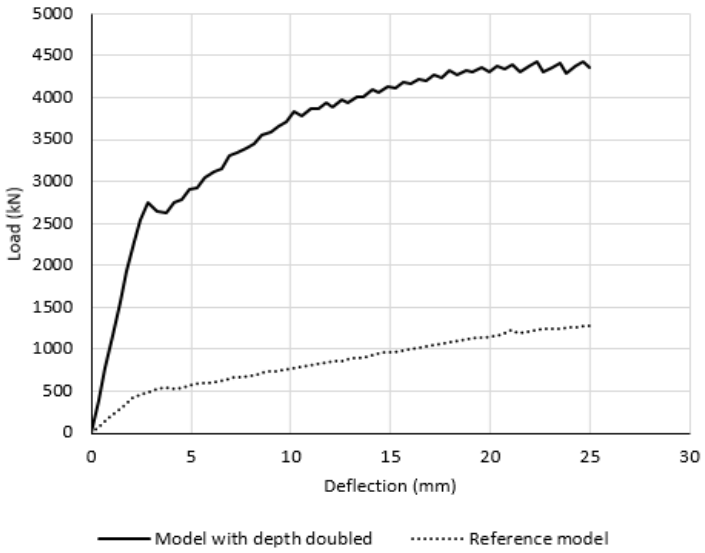

Figure 38 *Load deflection curve for the model with twice the depth compared with the reference model.*

4.2.3.1 One-way shear Resistance

The increase in effective depth of the slab caused an change in the location of the critical section and the distribution width.

According to the recommendations in Model Code 2010 (CEB-FIP, 2013)the distribution width is a function of the effective depth, and therefore for this model distribution width is changed as well. The value for one-way shear resistance was increased from 321 kN in the reference model to 686 kN in the model with increased depth. The value of applied load corresponding to this capacity of 686 kN was 2784kN.

The new proposed method for calculating the distribution width was also applied. The longitudinal distribution of shear force at an applied load of 2784 kN was obtained as shown in Figure 39.

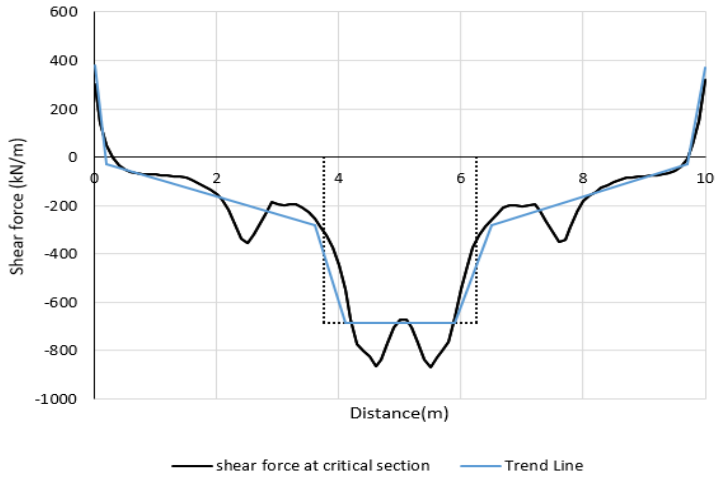

Figure 39 *Longitudinal distribution of one-way shear force, and determination of distribution width according to the proposed method.*

The horizontal part of the trend-line in Figure 39 gave a distribution width of 2m. The one-way shear resistance at the critical section was found to be 552kN. The corresponding value of applied load was obtained as 2272kN.

4.2.3.2 Punching shear resistance

The punching shear resistance was calculated using the same principle as outlined in section 3.4.3. The perimeter of the critical region was a function of the effective depth of the slab and with the increase in effective depth, the perimeter of critical section increased too. The value of punching shear resistance obtained was 3845kN. The curves used for the evaluation of punching shear are shown in Figure 40.

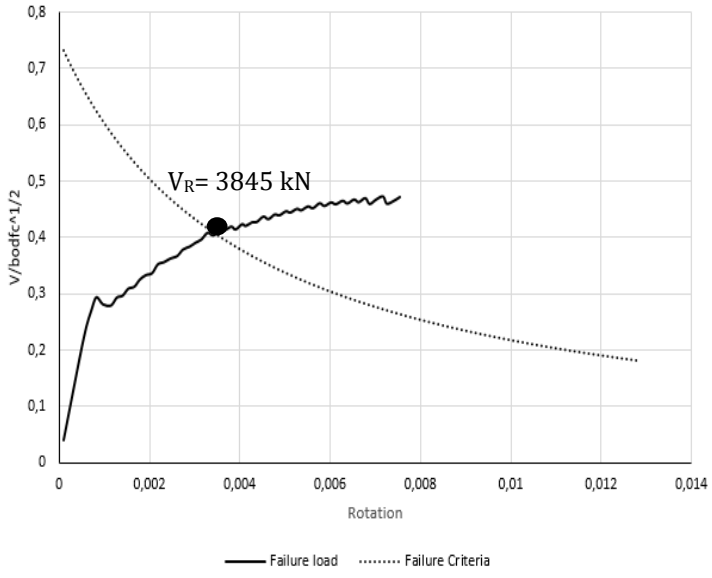

Figure 40 Evaluation of punching shear resistance.

4.2.3.3 Flexural resistance

From the non-linear analysis it was found that the rupture of top reinforcement took place at a load of 4730 kN. So the flexural resistance was 4730 kN.

4.2.4 Results and discussion

The results from the analysis of the model with twice the depth are shown in Table 12.

Table 12 Summary of results from the model with twice the depth.

Mode of failure	One-way shear resistance	Punching resistance	Flexural resistance
Applied load	2784kN (MC recommendation) 2272kN (proposed method)	3845kN	4730kN

Based on the values in the table it was concluded that one-way shear was the critical mode of failure. Figure 42summarizes the failure loads at different levels of analysis for this model and also compares them with the reference model.

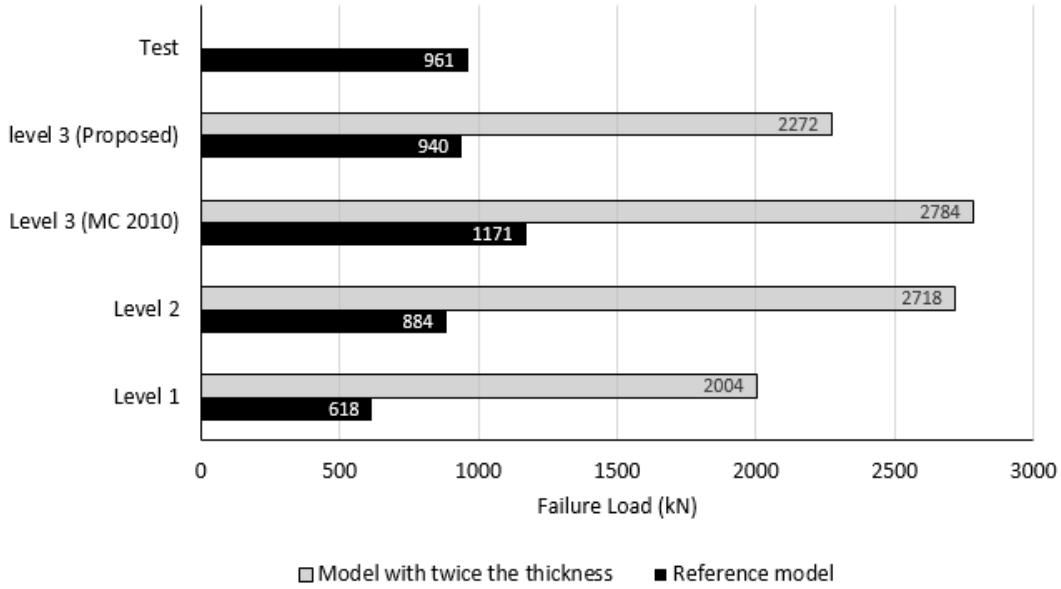

Figure 41 Multi-level structural assessment of slab with twice the depth. Results are compared with the reference model as well.

There was an increase in punching shear resistance at level III which was attributed to the increase in stiffness of the slab. The slab behaved much more stiff as compared to the reference model, which reduced the rotation values. Since the critical shear crack theory is based on the rotation of the slab, the punching shear resistance had a much higher value in this case.

4.3 Reinforcement ratios

The reinforcement in the transversal direction was increased such that the reinforcement ratio of the slab increased from 0.6% to 2.1%. The impact of this change on the structural response was then studied through a multi-level structural assessment.

4.3.1 Level I analysis

In level I analysis the one-way and punching shear resistance was obtained according to (Eurocode 2004). For detailed calculations see Appendix B. The results are summarized in Table 13.

Table 13 Summary of results from level I analysis of slab with high reinforcement ratio.

Mode of failure	One-way shear	Punching shear	Flexure
Applied load	436kN	1192kN	2095kN

4.3.2 Level II analysis

The applied load value for one way shear resistance was found to be1047kN.For the detailed method see section 3.3.2. The punching resistance value was unchanged. The flexural resistance value was evaluated using the method explained in section 3.3.4 and was found to be 1342kN.The results from level II analysis are summarized in Table 14.

Table 14 Summary of results from level II analysis of slab with high reinforcement ratio.

Mode of failure	One-way shear	Punching shear	Flexure
Applied load	1047kN	1192kN	1342kN

4.3.3 Level III analysis

For level III non-linear analysis of the model, a load deflection curve was obtained and compared against the load deflection curve of the reference model. They are shown in Figure 42.

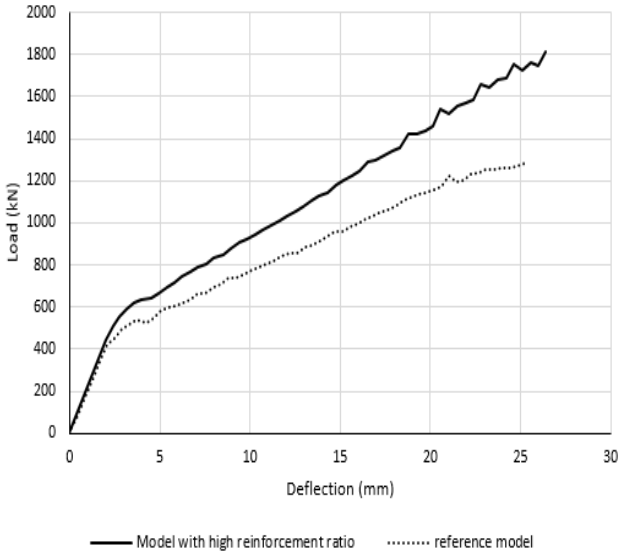

Figure 42 Load displacement curve of the model with high reinforcement ratio and the reference model.

It was seen that the models acted similarly in the linear phase but the model with higher reinforcement ratio acted stiffer in the cracked state, as was expected. The following section describes the evaluation of the resistances based on different failure criteria.

4.3.3.1 One-way shear Resistance

One-way shear resistance was calculated as per Model Code 2010 (CEB-FIP, 2013). Because of the change in reinforcement ratio, the shear resistance was slightly increased. According to recommendations in Model Code 2010 (CEB-FIP, 2013) the one-way shear resistance at the critical section increased from 321kN to 359kN. The corresponding applied load was calculated to be 1339kN for this model, which was 14 % higher as compared to the reference model applied load of 1171 kN.

According to the new method proposed, the distribution width was calculated as 2.1m and the one-way shear resistance at the critical section was evaluated to be 240kN. The corresponding value of applied load was 1108kN. Figure 43 shows the longitudinal shear force distribution for the applied load of 1339kN and also the linear trend line used in the evaluation of distribution width based on the new method proposed.

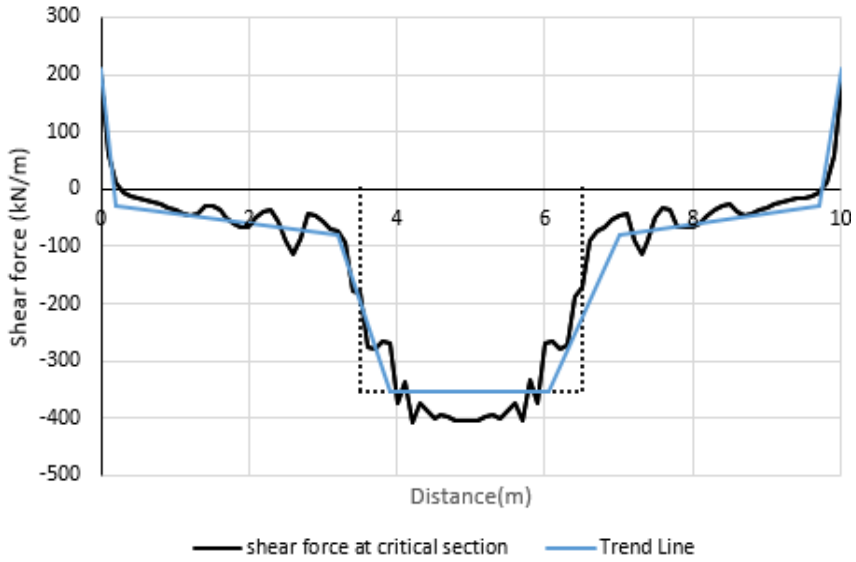

Figure 43 *Shear force distribution in the transversal direction when one way shear failure occurs.*

4.3.3.2 Punching Shear Resistance

The punching shear resistance was calculated using the same principle as outlined in section 3.4.3. The evlauation is shown in Figure 44. The control perimeter remained the same as was in the case of the referencec model since the effective depth of both the models was the same. However, since the model with higher reinforcement ratio offered much more resistance to deformation, the applied load calculated based on this critera was expectedly higher than the reference model. The failure load according to punching shear criteria had a value of 1520 kN which was 16 % higher than the reference model punching shear failure load of 1315 kN.

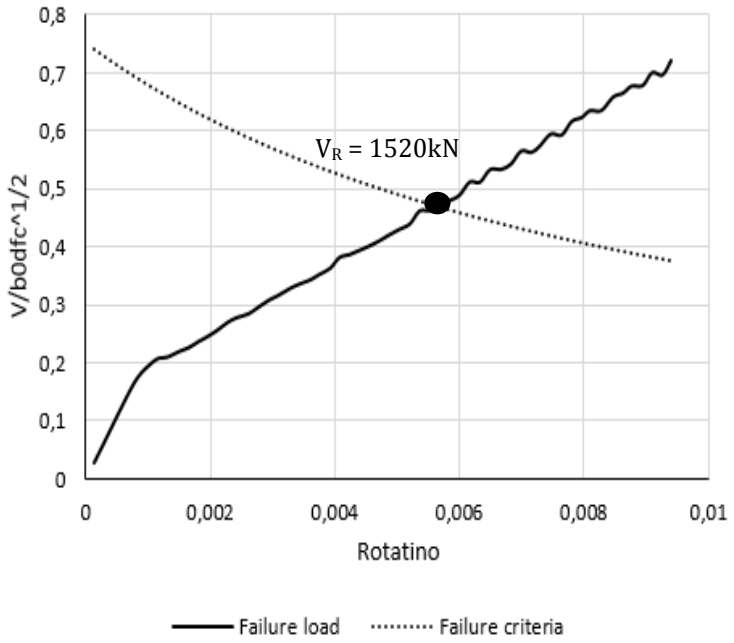

Figure 44 Calculation of punching shear capacity for model with high reinforcement ratio.

4.3.3.3 Flexural resistance

From the non-linear analysis, the load for which the top reinforcement ruptured was found to be 2890 kN. Additional material testing maybe required to evaluate the exact tensile strain when flexural failure occurs.

4.3.4 Results and discussion

The applied loads for the model with high reinforcement ratio (ρ=2.1%), based on different failure criteria are summarized in Table 15:

Table 15 Summary of the results from the model with high reinforcement ratio

Mode of failure	One-way shear resistance	Punching resistance	Flexural resistance
Applied load	1339kN (MC recommendation) 1108kN (proposed method)	1520kN	2890kN

It was seen that one-way shear capacity was the critical mode of failure. It was concluded that increasing the transversal reinforcement increased the load carrying capacity of the cantilever bridge deck slab. Figure 45 shows comparison between the failure loads at different levels of the analysis. For each level a comparison was made with the failure load from the reference model as well.

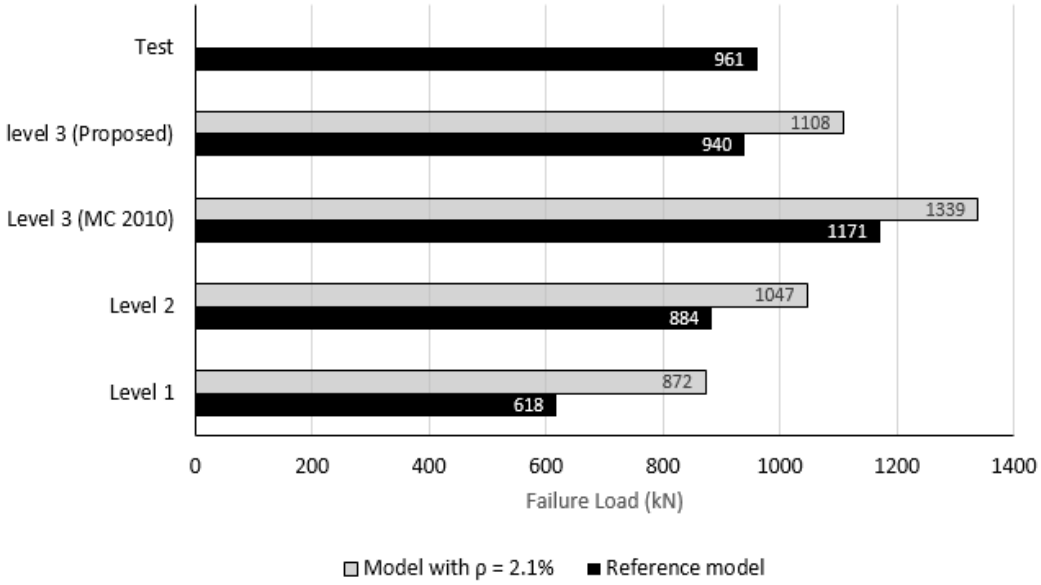

Figure 45 Comparison of the failure loads for different models.

It was observed that the mode of failure for the slab with high reinforcement ratio was one-way shear for all three levels of analysis. As expected the load carrying capacity of this model was higher than that of the reference model for all levels of analysis, owing to the increase in reinforcement ratio.

4.4 Influence of edge beams

Edge beams affect the structural response of a bridge cantilever in terms of distribution of shear flow as suggested in(Vaz Rodriguez 2007). It was suggested from the analysis of (Vaz Rodriguez 2007) that the load carrying capacity of the cantilever slab was a function of the stiffness of the edge beam. To study the influence of edge beams, the FE model was remodeled with an edge beam and a non-linear analysis was performed. The dimension and the reinforcement details of the edge beam were taken from the Stallbacka Bridge located outside Trollhättan, Sweden. The edge beams were reinforced, both longitudinally and transversally, with ribbed bars. The longitudinal reinforcement consisted of four bars Ø16 Ks60 in the upper part, two bars Ø16 Ks60 at the bottom, and one bar Ø16 Ks60 at mid-height of the cross-section. The transverse reinforcement consisted of Ø10 s300 Ks40. Ks 60 and Ks 40 are old Swedish notations for steel reinforcement with characteristic yield strength of 600 and 400 MPa, respectively(Lundgren *et al* 2014). Figure 46 shows the reinforcement detail as well as the FE model of the cantilever deck with edge beams.

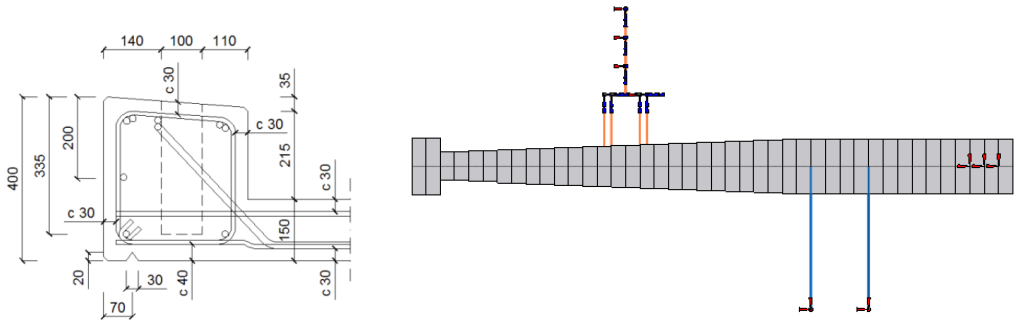

Figure 46 *Figure on the left shows the reinforcement detail taken from (Lundgren et al 2014). Figure on the right shows the FE-model used in this project with edge beam.*

4.4.1 Level I analysis

In level I analysis the one-way and punching shear resistance was obtained according to (Eurocode 2004). The results are summarized in Table 16 and detailed calculations can be found in Appendix B. Since (Eurocode 2004) had no specific recommendations for edge beams, same calculations and capacity values were used as that for the reference model. The detailed method can be seen in section 3.2.

Table 16 *Summary of level I analysis for slab with edge beams.*

Mode of failure	One-way shear	Punching shear	Flexure
Applied load	321kN	1108kN	1542kN

4.4.2 Level II analysis

The value of the one way shear resistance was obtained from linear analysis of the model according to the method outlined in section 3.3.2 and was found to be 952kN. Flexural resistance was found using the same method as section 3.3.4 and was found to be 1341kN. Punching resistance value was unchanged.

The results from level II analysis are summarized in Table 17.

Table 17 *Summary of results from level II analysis of the model with edge beams.*

Mode of failure	One-way shear	Punching shear	Flexure
Applied load	952kN	1108kN	1341kN

4.4.3 Level III analysis

A load versus deflection curve was plotted along with that of the reference model and is shown in the Figure 47. It was seen that the model with edge beam was much stiffer compared to the reference model.

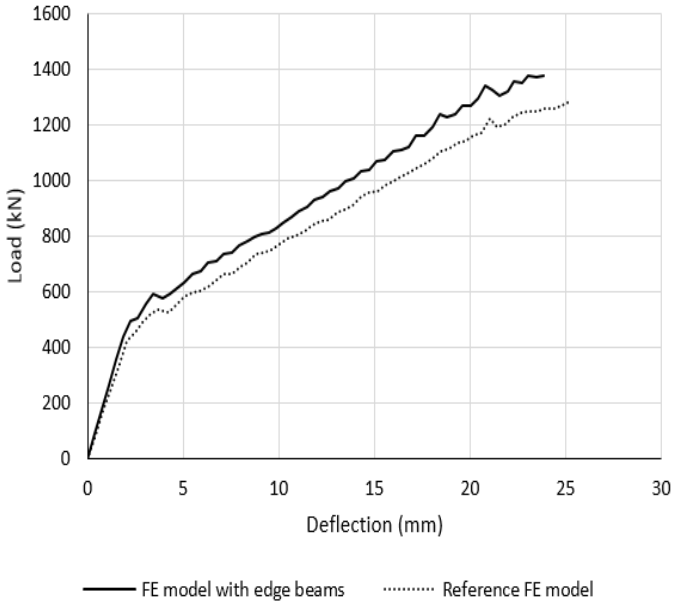

Figure 47 *Load deflection curve for the reference model and the model with edge beams.*

4.4.3.1 One-way shear Resistance

The one-way shear criteria remained the same as in the reference model (see section 3.4.2) as there was no provision in Model Code 2010 (CEB-FIP, 2013) to account for influence of edge beams. One-way shear resistance at the critical section had a value of 321kN according to Model Code 2010 (CEB-FIP, 2013). A non-linear analysis was performed on the model and the corresponding applied load was evaluated to be 1295 kN, which was 10% more than the one-way shear failure load of 1171 kN for the reference model.

According to the new method to evaluate the distribution width, the value of distribution width came out to be 2.2m. Figure 48 shows the longitudinal distribution of shear force in the slab at an applied load of 1295kN along with the linear trend line.

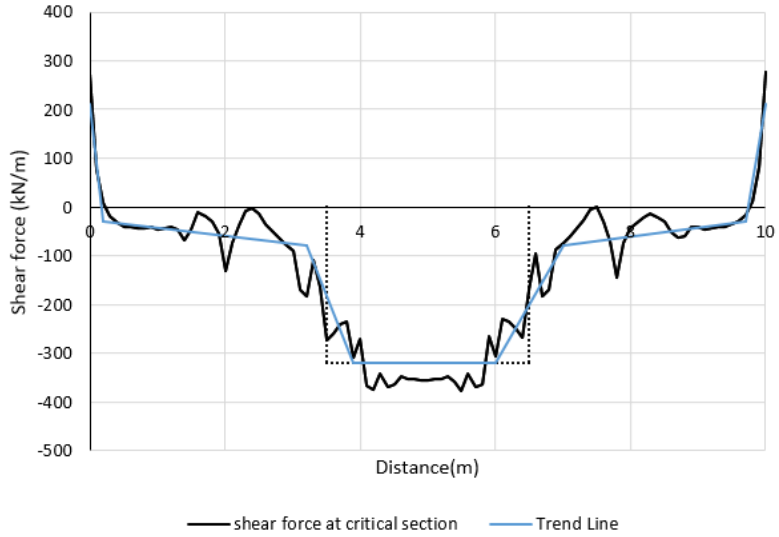

Figure 48 *Shear force distribution along the longitudinal section in the model with edge beams.*

According to the new method, the one-way shear resistance at the critical section was 250kN. The corresponding value of applied load was 1006kN.

4.4.3.2 Punching shear resistance

Punching shear resistance was calculated based on CSCT by Muttoni (see section 3.4.3). Since punching shear resistance is a function of the deformation of the slabs, the failure load under this criterion was evaluated to be 1366 kN which was slightly higher than thepunching shear capacity of 1315 kN for the reference model. The evaluation of punching shear capacity is shown in Figure 49.

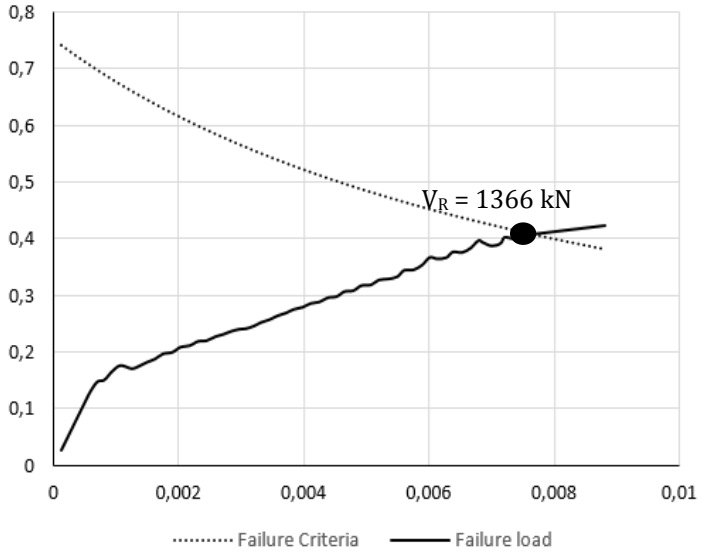

Figure 49 Evaluation of the punching shear resistance of the slab with edge beam.

4.4.3.3 Flexural resistance

The reinforcement strain values were extracted from the non-linear analysis and it was found that a load of 1980kN caused the rupture of reinforcement.

4.4.4 Results and discussion

The results from the analysis of the model with edge beams are shown in Table 18.

Table 18 Summary of level III analysis for slab with edge beams.

Mode of failure	One-way shear resistance	Punching resistance	Flexural resistance
Applied load	1295kN (MC recommendation) 1006kN (proposed method)	1366kN	1980kN

Figure 50 compares the failure load from the model with edge beams to that of the reference model and the experiment.

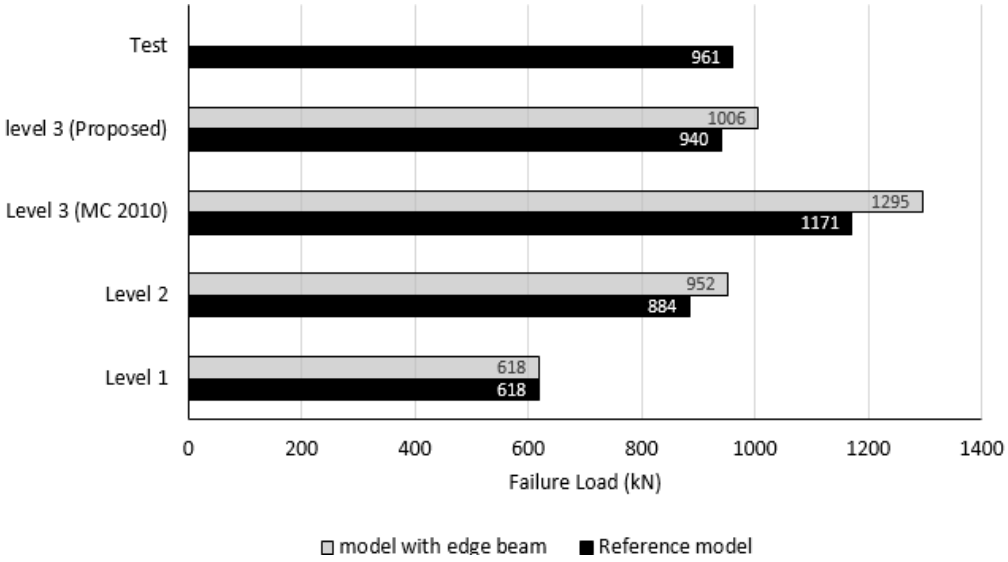

Figure 50 Comparison of failure loads between the model with edge beam and the reference model.

As mentioned before, presence of edge beams influences the shear flow within a cantilever slab. Figure 51shows the longitudinal shear force distribution at the critical section for the model with edge beam and the reference model, for the load of 1171kN. It was seen that the peak shear force value had been reduced due to the influence edge beams.

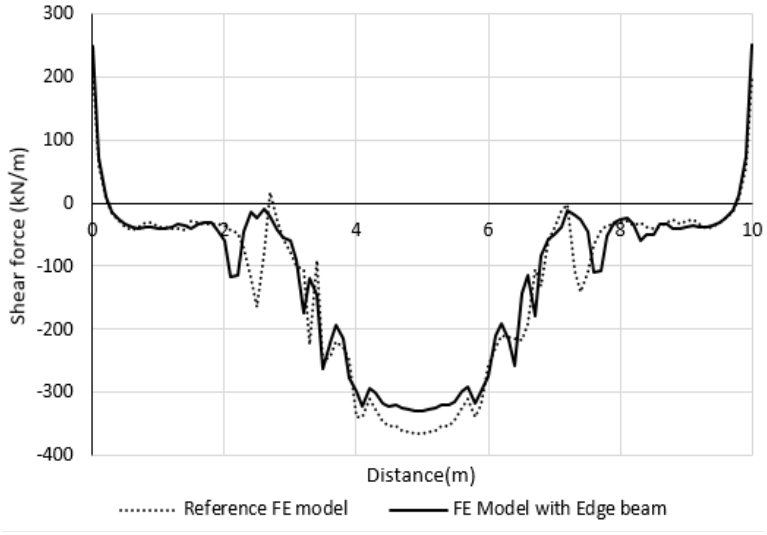

Figure 51 Longitudinal shear force distribution.

Apart from the shear flow, edge beams also influenced the moment distribution in the transversal direction. From the analysis by(Vaz Rodriguez 2007) it was suggested that the influence of edge beams reduced the maximum hogging moment at a distance of $d/2$ from the support line in the case of four point load. Figure 52 shows the longitudinal distribution of moment at a distance of $d/2$ in the case with two point loads and it was seen that the maximum hogging moment had been reduced as compared to the reference model for the applied load of 1171 kN.

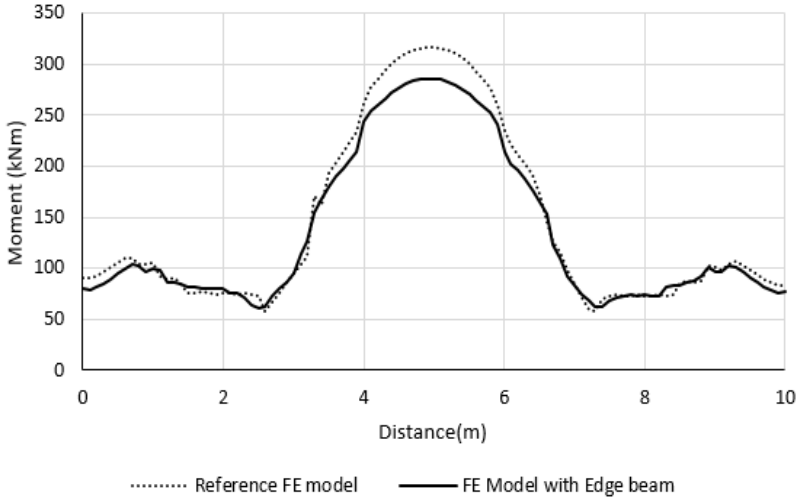

Figure 52 Moment distribution in the longitudinal direction.

5 Conclusions

- It was concluded on the basis of this project that the multi-level structural analysis provided a successively improved method of analysis of structures. The failure load with each level of assessment increased and also reflected the structural behavior of the slab better. However, the results from level III analysis for one-way shear resistance were on the unsafe side, as they over-estimated the load carrying capacity of the slab.
- One of the reasons of the over-estimation of one-way shear resistance in level III was the method for calculating distribution width according to Model Code 2010 (CEB-FIP, 2013).Model Code 2010 (CEB-FIP, 2013)gives recommendation for the distribution for the case of one point load only; there is no recommendations for two point loads acting close to one another. Therefore, the method used to calculate the distribution width for one point load was applied for the case of two point loads as well. This could have led to over-estimation of the distribution width and hence the one-way shear resistance was also over-estimated.
- The FE model for one of the slabs analyzed, slab DR2-A behaved much stiffer than the test specimen in the experiment(Vaz Rodriguez 2007). However, the load-deflection response for an FE analysis of slab DR2-A reported in (Vaz Rodriguez 2007)behaved as stiff as in the FE analysis made in this project. Consequently, it cannot be excluded that there was something different with the slab when the experiment was performed. Possibly, the pre-loading caused some changes in the slab that were not accounted for in the FE-model. But since the description was not sufficient in detail in (Vaz Rodriguez 2007) on this issue, no final conclusion could be drawn regarding why the FE-model behaved stiffer than the experiment.
- A new proposal for calculating the distribution width for one-way shear resistance at level III analysis was given in this project. The shear force distribution obtained from the non-linear analysis was used to determine a length over which it is more or less constant, that length was then used as the new distribution width. The proposed method gave lower values for the distribution width of the slabs in all the analysis performed. In the analysis for the reference model this resulted in a one-way shear resistance that was closer to the one obtained in the experiments (Vaz Rodriguez 2007). The method was also applied on all the parametric variations performed. It was seen that the longitudinal distribution of the shear force could successfully be used to calculate a distribution width value as recommended in the new proposal. However, the accuracy of the distribution width calculated was not verified through this project. Further investigations and/or experiments are required for evaluation of this proposal before it can be judged credible in general.
- Parametric studies revealed interesting results in terms of load carrying capacity and behavior of the structure. Table 19 summarizes the effects of each parametric variation. The load-carrying capacity, load distribution and failure mode of each parametric study were compared against that of the reference model, and any change in comparison to the reference model was indicated with a tick mark.

Table 19 Results of parametric variations as compared to the reference model for level III analysis.

Parametric variation	Load-carrying capacity	Load distribution	Failure mode
Reduced spring stiffness	✓	✓	✓
Depth doubled	✓		
Reinforcement ratio increased	✓		
Influence of edge beams	✓	✓	

The parametric studies performed in this master thesis helped predict the change in structural behavior when a certain parametric variation was applied. The table above shows that support stiffness influenced load carrying capacity, load distribution and failure mode of the structure. The depth and the reinforcement ratio only effected the load carrying capacity, while the presence of edge beams effected both the load carrying capacity and the load distribution.

6 References

BK, 2004. Boverkets handbok om betongkonstruktioner , BBK 04.

Broo, H., 2008. A guide to non-linear finite element modeling of shear and torsion in concrete bridges.

Ceb-Fip, 1993. CEB-FIP model code 1990. , p.460.

Eurocode, 2004. BS EN 1992-1-1:2004 - Eurocode 2: Design of concrete structures - Part 1-1: General rules and rules for buildings. *Eurocode 2*, 1(2004).

Eurocode, 2007. Eurocode 1.

Hakimi, P.S., 2012. Distribution of Shear Force in Concrete Slabs.

Hillerborg, A., 1996. Strip Method Design handbook.

Hordijk, 1991. Local approach to fatigue of concrete.

Kupryciuk& Georgeiv, 2013. Shear Distribution in Reinforced Concrete Bridge Deck Slabs.

Lundgren*et al*, 2014. Tests on anchorage of naturally corroded reinforcement in concrete. *Materials and Structures*.

MC, 2010. *Model Code for Concrete Structures*,

Muttoni, 2009. Punching Shear Strength of Reinforced Concrete Slabs. *ACI Structural Journal*, 105(105).

Pacoste*et al*, 2012. Recommendations for finite element analysis for the design of reinforced concrete slabs Costin Pacoste , Mario Plos , Morgan Johansson Department of Civil and Recommendations for finite element analysis for the design of concrete slabs Coordinator : Costi.

Plos, M., 2015. A Multi-level Strucutral Assessment Proposal for Reinforced Concrete Bridge Deck Slabs.

Rodrigues, 2007. Shear strength of reinforced concrete bridge deck slabs.

Thorenfeldt, 1987. Mechanical properties of high sterngth concrete and applications in design.

TNO DIANA User manual realease 9.4.4, 2011. TNO DIANA.

APPENDIX A

Calculations for reference model, slab DR2-A

1.1 Properties of top transversal reinfrocement in slab DR2-A

$L_{slab} := 10m$

$L_{slab.2} := 2.78m$

$Spacing := 75mm$

$Dia_{bar} := 14mm$

$Dia_{bar2} := 12mm$

$Spacing_2 := 150mm$

$$n_1 := \frac{L_{slab}}{Spacing_2} + 1 = 67.667$$

$$n_2 := \frac{L_{slab}}{Spacing} + 1 = 134.333$$

$$n_3 := \frac{L_{slab.2}}{Spacing_2} + 1 = 19.533$$

$$A_{steel.total} := \left(\frac{\pi \cdot Dia_{bar}^{2}}{4} \cdot n_2 \right) = 0.021 \cdot m^2$$ Amount of transversal steel

$$A_{steel.unit.length} := \frac{A_{steel.total}}{L_{slab}} = 2.068 \times 10^{-3}\, m$$

$$A_{steel.unit.length.2} := \frac{\frac{\pi \cdot Dia_{bar2}^{2}}{4} \cdot n_3}{L_{slab.2}} = 7.947 \times 10^{-4}\, m$$ Amount of longitudnal steel

1.2 LEVEL I Analysis

The average effective depth of the slab is evaluated by subtracting value of the cover and diameter reinforcement from one side.

$$d_1 := \frac{(0.19\text{m} - 0.03\text{m} - 0.02\text{m}) + (0.38\text{m} - 0.03\text{m} - 0.02\text{m})}{2} = 0.235\,\text{m}$$

$c_1 := 300\text{mm}$ Dimension of area of load application

$\gamma_c := 1.5$ Safety factor for concrete

$f_{ck} := 40$ Compressive strength of concrete used in slab DR2

One way shear resistance according to EC2

Calculation of the location of critical section

$c_1 = 0.3\,\text{m}$

$y_{cs} := \frac{c_1 + d_1}{2} = 0.267\,\text{m}$ According to the recommedation in Pacoste

$b_w := \min\left(7 \cdot d_1 + c_1, 10 \cdot d_1 + 1.3 \cdot y_{cs}\right) = 1.945\,\text{m}$

$b_w = 1.945\,\text{m}$

$C_{Rd.c} := \frac{0.18}{\gamma_c} = 0.12$

$k := 1 + \sqrt{\frac{200\text{mm}}{d_1}} = 1.923$ k is a factor depending on effective depth. It is taken according to EC2

$\rho_1 := 0.006$ Given in the properties of the slab

$$V_{Rd.c} := \left[C_{Rd.c} \cdot k \cdot \left(100 \cdot \rho_1 \cdot f_{ck}\right)^{\frac{1}{3}}\right] \cdot b_w \cdot d_1\,\text{MPa} = 304.167 \cdot \text{kN}$$

$$v_{min} := \left(0.035 \cdot k^{\frac{3}{2}} \cdot \sqrt{f_{ck}}\right) \cdot b_w \cdot d_1 \cdot 1\text{MPa} = 269.709 \cdot \text{kN}$$ So OK!

Punching shear resistance according to EC2

For punching shear the average depth flexural depth of the slab is used as in the case of one way shear

$d_{punch} := d_1 = 0.235\,m$

Perimeter of the critical section for punching

$slab_{width.1} := \left(c_1 + 0.9m + 4 \cdot d_{punch}\right) = 2.14\,m$

$slab_{width} := 1.48m + 2 \cdot d_{punch} = 1.95\,m$

Calculate reinforcement ratio in both x and y direction

For bars lying along the x-axis

$A_{steel.x} := \frac{A_{steel.total}}{L_{slab}} \cdot \left(c_1 + 2 \cdot 3 \cdot d_{punch}\right) = 3.536 \times 10^{-3}\,m^2$

According to EC2 section 6.4.4, the reinforcement is taken at a distance of c+3d on each side

$\rho_y := \frac{A_{steel.x}}{d_{punch} \cdot 1m} = 0.015$

For bars lying along the y-axis

$dia_{bar.2} := 12mm$

$bar_{spacing.y} := 150mm$

$L_{slab.2} := 2.78m$

$n_{bars.y} := \frac{L_{slab.2}}{bar_{spacing.y}} + 1 = 19.533$

$A_{steel.total.2} := n_{bars.y} \cdot \frac{\pi \cdot dia_{bar.2}^2}{4} = 2.209 \times 10^{-3}\,m^2$

$A_{steel.y} := \frac{A_{steel.total.2}}{L_{slab.2}} \cdot \left(c_1 + 2 \cdot 3 \cdot d_{punch}\right) = 1.359 \times 10^{-3}\,m^2$

$\rho_x := \frac{A_{steel.y}}{d_{punch} \cdot 1m} = 5.782 \times 10^{-3}$

$\rho_2 := \sqrt{\rho_x \cdot \rho_y} = 9.328 \times 10^{-3}$

Control perimeter for punching shear

$l_1 := c_1 + 0.9m + 4.d_{punch} = 2.14\,m$

The perimeter of punching shear is taken for the case where load is close to the edge according to EC2. Perimeter is taken as 2d from each side

$l_2 := 1.48m + 2\cdot d_{punch} + \frac{c_1}{2} = 2.1\,m$

$l_3 := c_1 + 4\cdot d_{punch} = 1.24\,m$

$u := 2\cdot l_2 + l_1 = 6.34\,m$

$u_2 := 2\cdot l_3 + 2\cdot l_1 = 6.76\,m$

$V_{Rd.punching} := \left[C_{Rd.c}\cdot k\cdot\left(100\cdot\rho_2\cdot f_{ck}\right)^{\frac{1}{3}}\right]\cdot\left(u\cdot d_{punch}\right)\cdot MPa = 1.149\times 10^{3}\cdot kN$

$V_{Rd.punching.2} := \left[C_{Rd.c}\cdot k\cdot\left(100\cdot\rho_2\cdot f_{ck}\right)^{\frac{1}{3}}\right]\cdot\left(u_2\cdot d_{punch}\right)MPa = 1.225\times 10^{6}\,N$

Moment resistance of the slab according to yield line method

Determine the depth of the concrete block

$b := 1m$

$d := 0.285m$ Use an average value for the total depth

Assume value of concrete cover on either side of 30mm

$cover := 30mm$

$A_{s.1} := \frac{A_{steel.total}}{L_{slab}}\cdot m = 2.068\times 10^{-3}\,m^2$ Top reinforcement

$A_{s2} := \frac{\frac{\pi\cdot Dia_{bar2}^{\,2}}{4}\cdot n_1}{L_{slab}}\cdot m = 7.653\times 10^{-4}\,m^2$ Bottom reinforcement

Assuming that the tension steel yields:

$f_y := 515MPa$ Yield strain top tensile reinforcement

$E_s := 200GPa$

$\varepsilon_{s1} := \frac{f_y}{E_s} = 2.575\times 10^{-3}$

$$centroid := \frac{cover \cdot A_{s.1} + \frac{d}{2} \cdot (b \cdot d) + (d - cover) \cdot A_{s2}}{A_{s.1} + d \cdot b + A_{s2}} = 0.142\,m$$ Centroid of the section

$$\varepsilon_{s.2} := 0.003 \frac{(d - centroid - cover)}{(d - centroid)} = 2.371 \times 10^{-3}$$ Less than yield strain, bottom reinforcement

$$\sigma_{compression.steel} := \varepsilon_{s.2} \cdot E_s = 474.134 \cdot MPa$$ Less than yield stress of 515 MPa

$$a := \frac{\left(\left(A_{s.1} \cdot f_y - A_{s2} \cdot \sigma_{compression.steel}\right)\right)}{0.85 \cdot f_{ck} \cdot b \cdot MPa} = 0.021\,m$$ Height of concrete compression block

$$\sigma_{tension.steel} := \varepsilon_{s1} \cdot E_s = 515 \cdot MPa$$

Concrete-steel and steel-steel couple used to give the resistance

$$m_{y.top} := \left(\sigma_{tension.steel} \cdot A_{s.1} - \sigma_{compression.steel} \cdot A_{s2}\right)\left(d - \frac{a}{2}\right) \ldots + \sigma_{compression.steel} \cdot A_{s2} \cdot (d - 2cover) = 274.496 \cdot kN \cdot m$$

Now top reinforcement in x direction:

$$A_{steel.total.x} := A_{steel.total.2} = 2.209 \times 10^{-3}\,m^2$$

$$A_{steel.x} := \frac{A_{steel.total.x}}{L_{slab.2}} \cdot 1m = 7.947 \times 10^{-4}\,m^2$$

$$centroid_x := \frac{cover \cdot A_{steel.x} + \frac{d}{2} \cdot (b \cdot d) + (d - cover) \cdot A_{steel.x}}{A_{steel.x} + d \cdot b + A_{steel.x}} = 0.143\,m$$ Centroid of the section

$$\varepsilon_{s.2.x} := 0.003 \frac{\left(d - centroid_x - cover\right)}{\left(d - centroid_x\right)} = 2.368 \times 10^{-3}$$ Less than yield strain, bottom reinforcement

$\sigma_{compression.steel.x} := \varepsilon_{s.2.x} \cdot E_s = 473.684 \cdot MPa$ Less than yield stress of 515 MPa

$a_2 := \frac{\left(\left(A_{steel.x} \cdot f_y - A_{steel.x} \cdot \sigma_{compression.steel}\right)\right)}{0.85 \cdot f_{ck} \cdot b \cdot MPa} = 9.551 \times 10^{-4}\,m$ Height of concrete compression block

Concrete-steel and steel-steel couple used to give the resistance

$m_{x.top} := \left(\sigma_{tension.steel} \cdot A_{steel.x} - \sigma_{compression.steel} \cdot A_{steel.x}\right)\left(d - \frac{a_2}{2}\right) \ldots = 94.015 \cdot kN \cdot m$
$+ \sigma_{compression.steel} \cdot A_{steel.x} \cdot (d - 2.cover)$

$m_{x.bottom} := m_{x.top}$

$m_{y.bottom} := m_{x.bottom}$

YIELD LINE METHOD

Assume a value for the displacement under the point load is taken as 1m

$b_{yield} := 1.2m$

$a_{load} := 1.3m$

$L_{slab.2} = 2.78\,m$

$f_{slab} := a_{load} \cdot \tan(10deg) = 0.229\,m$

$e_{slab} := a_{load} \cdot \tan(32deg) = 0.812\,m$

$c_{slab} := a_{load} \cdot \tan(32deg) = 0.812\,m$

Yield line number 1:

$yield_{one} := m_{y.top} \cdot b_{yield} \cdot \frac{1}{a_{load}} = 253.381 \cdot kN \cdot m$

Yield line number 2:

$$yield_{two} := 2 \cdot m_{x.top} \cdot L_{slab.2} \cdot \frac{1}{c_{slab}} + 2 \cdot m_{y.top} \cdot e_{slab} \cdot \frac{1}{a_{load}} = 986.532 \cdot kN \cdot m$$

Yield line number 3:

$$yield_{three} := 2 \cdot m_{x.bottom} \cdot a_{load} \cdot \frac{1}{c_{slab}} + 2 \cdot m_{y.bottom} \cdot f_{slab} \cdot \frac{1}{a_{load}} = 334.065 \cdot kN \cdot m$$

$$Load_{flexure} := \frac{yield_{one} + yield_{two} + yield_{three}}{1m} = 1.574 \times 10^{3} \cdot kN$$

1.3 LEVEL II Analysis

The applied load value for one way shear failure would be extracted using linear finite element analysis of the slab.

The moment capacity for a unit width of the slab in the y direction was used to evlauated the flexura capacity in level II analysis.

1.4 LEVEL III Analysis

One-way shear resistance according to model code 2010

$d_3 := 0.35m = 0.35\,m$ The effective depth of slab at the deepest section which will be used to evaluate distirbution width.

$d_z := d_1 = 0.235\,m$ Average effective depth of the slab that is used to calculate the one way shear resistance.

$z := d_z - 0.03m - 0.04m = 0.165\,m$ Distance between reinforcements so cover and bar diameters from other side is also reduced

$\gamma_c = 1.5$ Safety factor for concrete

According to model code 2010 section 7.3.1 the effective depth at deepest section (d.3) is used to evaluate location of critical section. The distance between reinforcements (z) is used to evalaute the resistance value

.

No axial force exists so level I approximation is used for kv

$$k_{v.1} := \frac{180mm}{1000mm + 1.25z} = 0.149$$ kdg is taken as 1 since aggregate size is 16mm.

$d_{cr} := 1.3m - d_3 = 0.95\,m$ Location of the critical section

$b_{w.2} := 0.9m + 2 \cdot d_{cr} \cdot \tan(45deg) + 0.3m = 3.1\,m$

The control section is taken at a distance of min (d, a/2) from the support.

$$V_{Rd.c.shear} := k_{v.1} \cdot \frac{\sqrt{f_{ck}} \cdot MPa}{\gamma_c} \cdot z \cdot b_{w.2} = 321.825 \cdot kN$$

A new method was proposed that changed the vlaue of bw. The resistance according to the new method is as follows

$$V_{Rd.c.shear.proposedmethod} := k_{v.1} \cdot \frac{\sqrt{f_{ck}} \cdot MPa}{\gamma_c} \cdot z \cdot 2.2m = 228.392 \cdot kN$$

Punching shear according to model code 2010 (this is for level III analysis)

Evaluated using excel and results from non linear analysis. The control section perimeter used is calculated below:

$d_5 := d_1 = 0.235\,m$

$c_1 = 0.3\,m$

$l_3 := 0.9m + d_5 + c_1 = 1.435\,m$

This is an approximation since in reality the critical section is not a perfect rectangle.

$l_4 := c_1 + 0.5 \cdot d_5 = 0.417\,m$

$b_0 := 2 \cdot (l_4) + l_3 = 2.27\,m$

$b_0 \cdot d_5 \cdot \sqrt{40}\,MPa = 3.374 \times 10^6\,N$

This value is used in the calculation of punching shear strength.

Spring of stiffness

Same value for bdfc as in the original case

APPENDIX B

PARAMETRIC STUDY

2.1 SPRING STIFFNESS REDUCED

All the calculated resistnces will remain the same

2.2 DEPTH OF THE SLAB DOUBLED

LEVEL I Analysis

The average effective depth of the slab is evaluated by subtracting value of the cover and diameter reinforcement from one side.

$$d_{1.doubled} := \frac{(0.38m - 0.03m - 0.02m) + (0.76m - 0.03m - 0.02m)}{2} = 0.52\,m$$

One way shear resistance according to EC2

Calculation of the location of critical section

$c_1 = 0.3\,m$

$$y_{cs.doubled} := \frac{c_1 + d_{1.doubled}}{2} = 0.41\,m$$

According to the recommedation in Pacoste

$$b_{w.doubled} := \min\left(7 \cdot d_{1.doubled} + c_1, 10 \cdot d_{1.doubled} + 1.3 \cdot y_{cs.doubled}\right) = 3.94\,m$$

$b_{w.doubled} = 3.94\,m$

$$k_{doubled} := 1 + \sqrt{\frac{200mm}{d_{1.doubled}}} = 1.62$$

k is a factor depending on effective depth. It is taken according to EC2

$$\rho_{1.doubled} := \frac{A_{steel.unit.length}}{d_{1.doubled}} = 3.977 \times 10^{-3}$$ Given in the properties of the slab

$$V_{Rd.c.doubled} := \left[C_{Rd.c} \cdot k_{doubled} \cdot \left(100 \cdot \rho_{1.doubled} \cdot f_{ck}\right)^{\frac{1}{3}}\right] \cdot b_{w.doubled} \cdot d_{1.doubled}\,MPa = 1.002 \cdot MN$$

$$v_{min.doubled} := \left(0.035 \cdot k_{doubled}^{\frac{3}{2}} \cdot \sqrt{f_{ck}}\right) \cdot \left(b_{w.doubled} \cdot d_{1.doubled}\right) \cdot 1MPa = 935.276 \cdot kN$$

Punching shear resistance according to EC2 So OK!

For punching shear the average depth flexural depth of the slab is used as in the case of one way shear

$$d_{punch.doubled} := d_{1.doubled} = 0.52\,m$$

Perimeter of the critical section for punching

Calculate reinforcement ratio in both x and y direction

For bars lying along the x-axis

According to EC2 section 6.4.4, the reinforcement is taken at a distance of c+3d on each side

$$A_{steel.x.doubled} := \frac{A_{steel.total}}{L_{slab}} \cdot \left(c_1 + 2 \cdot 3 \cdot d_{punch.doubled}\right) = 7.072 \times 10^{-3}\,m^2$$

$$\rho_{y.doubled} := \frac{A_{steel.x.doubled}}{d_{punch.doubled} \cdot 1m} = 0.014$$

For bars lying along the y-axis

$$A_{steel.y.doubled} := \frac{\frac{\pi \cdot Dia_{bar2}^{2}}{4} \cdot n_3}{L_{slab.2}} \cdot \left(c_1 + 2 \cdot 3 \cdot d_{punch.doubled}\right) = 2.718 \times 10^{-3}\,m^2$$

$$\rho_{x.doubled} := \frac{A_{steel.y.doubled}}{d_{punch.doubled} \cdot 1m} = 5.226 \times 10^{-3}$$

$$\rho_{2.db} := \sqrt{\rho_{x.doubled} \cdot \rho_{y.doubled}} = 8.431 \times 10^{-3}$$

Control perimeter for punching shear

$l_{1.doubled} := c_1 + 0.9m + 4.d_{punch.doubled} = 3.28\,m$

The perimeter of punching shear is taken for the case where load is close to the edge according to EC2. Perimeter is taken as 2d from each side

$k_{doubled.punch} := 1 + \sqrt{\frac{200mm}{d_{punch.doubled}}} = 1.62$

$l_{2.doubled} := 1.48m + 2 \cdot d_{punch.doubled} = 2.52\,m$

$u_{db} := 2 \cdot l_{2.doubled} + l_{1.doubled} = 8.32\,m$

$V_{Rd.punching.doubled} := \left[C_{Rd.c} \cdot k_{doubled} \cdot \left(100 \cdot \rho_{2.db} \cdot f_{ck}\right)^{\frac{1}{3}} \right] \cdot \left(u_{db} \cdot d_{punch.doubled}\right) \cdot MPa = 2.718 \cdot MN$

LEVEL II ANALYSIS

Same resistance values as level I analysis.

LEVEL III ANALYSIS

One way shear resistance according to Model Code 2010

The depth of the slab is doubled, so the thicker end is now 0.76m and the narrow end of the slab is 0.38m high.

$cover_2 := 0.03m$

$d_{deep} := 0.76m - cover_2 - 0.02m = 0.71\,m$

d labelled in the model code as the thicker en d in a tapered slab.

$z_2 := d_{deep} - cover_2 - 0.014m = 0.666\,m$

z is calculated as the centre to centre distance between the reinforcement layers

$k_{v.deep} := \frac{180mm}{1000mm + 1.25 \cdot z_2} = 0.098$

Since there is no axial force and the aggregate size is more than 10mm.

$d_{cr.2} := 0.65m$

If d is too large then location of critical section is taken as half the distance between support and load

$b_{w.deep} := 0.9m + 2 \cdot 0.65m \cdot \tan(45deg) + 0.3m = 2.5\,m$

The control section is taken at a distance of min (d, a/2) from the support. In this case it would be a/2. Since d is larger we take a/2

$$V_{Rd.c.shear.deep} := k_{v.deep} \cdot \frac{\sqrt{f_{ck}} \cdot MPa}{\gamma_c} \cdot z_2 \cdot b_{w.deep} = 689.575 \cdot kN$$

Resistance according to the new proposed method

$$V_{Rd.c.shear.deep.pm} := k_{v.deep} \cdot \frac{\sqrt{f_{ck}} \cdot MPa}{\gamma_c} \cdot z_2 \cdot 2.m = 551.66 \cdot kN$$

Punching shear resistance

$$d_4 := \frac{\left(0.76m - cover_2 - 0.014m\right) + \left(0.38m - cover_2 - 0.014m\right)}{2} = 0.526\,m$$

$$l_5 := c_1 + 0.9m + d_4 = 1.726\,m$$

$$l_6 := c_1 + 0.5d_4$$

$$b_{0.deep} := 2 \cdot \left(l_6\right) + l_5 = 2.852\,m$$

Moment resistance

Determine the depth of the concrete block

$$b = 1\,m$$

$d_{deep.m} := 0.57m$ Use an average value for the effective depth

Assume value of concrete cover on either side of 40mm

$A_{s.1} = 2.068 \times 10^{-3}\,m^2$ Top transversal reinforcement

$A_{s2} = 7.653 \times 10^{-4}\,m^2$ Bottom transversal reinforcement

Assuming that the tension steel yields:

$\varepsilon_{s1} = 2.575 \times 10^{-3}$ Yield strain top tensile reinforcement

Centroid of the section

$$centroid_{deep} := \frac{cover_2 \cdot A_{s.1} + \frac{d_{deep.m}}{2} \cdot \left(b \cdot d_{deep.m}\right) + \left(d_{deep.m} - cover_2\right) \cdot A_{s2}}{A_{s.1} + d_{deep.m} \cdot b + A_{s2}} = 0.284\,m$$

$$\varepsilon_{s.2.deep} := 0.003 \frac{\left(d_{deep.m} - centroid_{deep} - cover_2\right)}{centroid_{deep}} = 2.696 \times 10^{-3}$$ More than yield stress

$$\varepsilon_{s.2.deep.actual} := 2.575 \times 10^{-3}$$

$$\sigma_{compression.steel.deep} := \varepsilon_{s.2.deep.actual} \cdot E_s = 515 \cdot MPa$$ Less than yield stress of 515 MPa

$$a_{deep} := \frac{\left(\left(A_{s.1} \cdot f_y - A_{s2} \cdot \sigma_{compression.steel.deep}\right)\right)}{0.85 \cdot f_{ck} \cdot b \cdot MPa} = 0.02\,m$$ Height of concrete compression block

$$\sigma_{tension.steel.deep} := \varepsilon_{s1} \cdot E_s = 515 \cdot MPa$$

Concrete-steel and steel-steel couple used to give the resistance

$$m_{y.top.deep} := \begin{pmatrix} \sigma_{tension.steel.deep} \cdot A_{s.1} \cdots \\ + -\sigma_{compression.steel.deep} \cdot A_{s2} \end{pmatrix} \cdot \left(d_{deep.m} - \frac{a_{deep}}{2}\right) \ldots + \sigma_{compression.steel.deep} \cdot A_{s2} \cdot \left(d_{deep.m} - 2cover_2\right) = 576.767 \cdot kN \cdot m$$

Now top reinforcement in x direction:

In this direction both the top and bottom steel have same area per unit length

$$A_{steel.total.x} = 2.209 \times 10^{-3}\,m^2$$

$$A_{steel.x} = 7.947 \times 10^{-4}\,m^2$$

$$centroid_{x.2} := \frac{cover_2 \cdot A_{steel.x} + \frac{d_{deep.m}}{2} \cdot \left(b \cdot d_{deep.m}\right) + \left(d_{deep.m} - cover_2\right) \cdot A_{steel.x}}{A_{steel.x} + d_{deep.m} \cdot b + A_{steel.x}} = 0.285\,m$$

$$\varepsilon_{s.2.x.deep} := 0.003 \frac{\left(d_{deep.m} - centroid_{x.2} - cover_2\right)}{\left(centroid_{x.2}\right)} = 2.684 \times 10^{-3}$$ Less than yield strain, bottom reinforcement

$$\varepsilon_{s.2.x.deep.actual} := 2.575 \times 10^{-3}$$

$$\sigma_{compression.steel.x.deep} := \varepsilon_{s.2.x.deep.actual} \cdot E_s = 515 \cdot MPa$$ Less than yield stress of 515 MPa

Height of concrete compression block

$$a_{2.deep} := \frac{\left(\left(A_{steel.x} \cdot f_y\right)\right)}{0.85 \cdot f_{ck} \cdot b \cdot MPa} = 0.012\,m$$

Concrete-steel and steel-steel couple used to give the resistance

$$m_{x.top.deep} := \begin{pmatrix} \sigma_{tension.steel.deep} \cdot A_{steel.x} \cdots \\ +-\sigma_{compression.steel.x.deep} \cdot A_{steel.x} \\ +\left[\sigma_{compression.steel.x.deep} \cdot A_{steel.x} \cdot \left(d_{deep.m} - 2cover_2\right)\right] \end{pmatrix} \left(d_{deep.m} - \frac{a_{2.deep}}{2}\right) \ldots = 208.719 \cdot kN \cdot m$$

$$m_{x.bottom.deep} := m_{x.top.deep}$$

$$m_{y.bottom.deep} := m_{x.bottom.deep}$$

YIELD LINE METHOD

Assume a value for the displacement under the point load is taken as 1m

$$b_{yield} = 1.2\,m$$

$$a_{load} = 1.3\,m$$

$$L_{slab.2} = 2.78\,m$$

$$f_{slab} := a_{load} \cdot \tan(10deg) = 0.229\,m$$

$$e_{slab} := a_{load} \cdot \tan(32deg) = 0.812\,m$$

$$c_{slab} := a_{load} \cdot \tan(32deg) = 0.812\,m$$

Yield line number 1:

$$yield_{one.deep} := m_{y.top.deep} \cdot b_{yield} \cdot \frac{1}{a_{load}} = 532.4 \cdot kN \cdot m$$

Yield line number 2:

$$yield_{two.deep} := 2 \cdot m_{x.top.deep} \cdot L_{slab.2} \cdot \frac{1}{c_{slab}} + 2 \cdot m_{y.top.deep} \cdot e_{slab} \cdot \frac{1}{a_{load}} = 2.149 \times 10^3 \cdot kN \cdot m$$

Yield line number 3:

$$yield_{three.deep} := 2 \cdot m_{x.bottom.deep} \cdot a_{load} \cdot \frac{1}{c_{slab}} + 2 \cdot m_{y.bottom.deep} \cdot f_{slab} \cdot \frac{1}{a_{load}} = 741.645 \cdot kN \cdot m$$

$$Load_{flexure.deep} := \frac{yield_{one.deep} + yield_{two.deep} + yield_{three.deep}}{1m} = 3.423 \times 10^{3} \cdot kN$$

2.3 HIGH REINFORCEMENT RATIO (2.1%)

Verification of the reinforcement ratio of slab DR1-A

With increased reinforcement ratio the transversal reinforcement in top and bottom of the slab is changed such that the total reinforcement ratio comes up to 0.021. The reinforcement in the longitudnal direction would remain the same

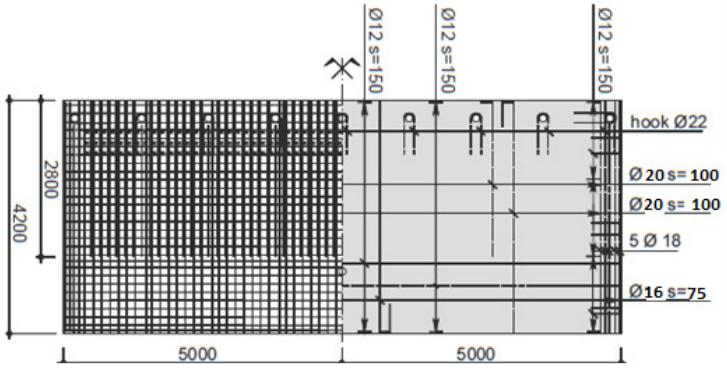

Verification that the reinforcement ratio is 2.1

Reinforcement lying in x direction

$$Dia_{bar.top.x} := 20mm$$

$$spacing_{bar.top.x} := 100mm$$

$$Dia_{bar.bottom.x} := 16mm$$

$$spacing_{bar.bottom.x} := 75mm$$

$$L_{slab} = 10\,m$$

$$A_{steel.top.one.bar} := \frac{\pi \cdot Dia_{bar.top.x}^{2}}{4} = 3.142 \times 10^{-4}\,m^{2}$$

$$No_{bars} := \frac{L_{slab}}{spacing_{bar.top.x}} + 1 = 101$$

$$A_{steel.total.top} := A_{steel.top.one.bar} \cdot No_{bars} = 0.032\,m^{2}$$

$$Ratio_1 := \frac{A_{steel.total.top}}{L_{slab} \cdot 285mm} = 0.011$$

$$A_{steel.bottom} := \frac{\pi \cdot Dia_{bar.bottom.x}^{2}}{4} = 2.011 \times 10^{-4}\,m^2$$

$$No_{bars.bottom} := \frac{L_{slab}}{spacing_{bar.bottom.x}} + 1 = 134.333$$

$$A_{steel.total.bottom} := No_{bars.bottom} \cdot A_{steel.bottom} = 0.027\,m^2$$

$$Ratio_2 := \frac{A_{steel.total.bottom}}{L_{slab} \cdot 285mm} = 9.477 \times 10^{-3}$$

$$Ratio := Ratio_1 + Ratio_2 = 0.021$$

LEVEL I Analysis

The average effective depth of the slab is evaluated by subtracting value of the cover and diameter reinforcement from one side.

$$d_{z.hr} := \frac{(0.38 - 0.03 - 0.028) + (0.19 - 0.03 - 0.028)}{2} m = 0.227\,m$$

One way shear resistance according to EC2

Calculation of the location of critical section

$c_1 = 0.3\,m$

$$y_{cs.rr} := \frac{c_1 + d_{z.hr}}{2} = 0.263\,m$$

According to the recommedation in Pacoste

$$b_{w.rr} := \min\left(7 \cdot d_{z.hr} + c_1, 10 \cdot d_{z.hr} + 1.3 \cdot y_{cs.rr}\right) = 1.889\,m$$

$b_{w.rr} = 1.889\,m$

$$k_{rr} := 1 + \sqrt{\frac{200mm}{d_{z.hr}}} = 1.939$$

k is a factor depending on effective depth. It is taken according to EC2

$\rho_{rr} := 0.021$

Given in the properties of the slab

$$V_{Rd.c.rr} := \left[C_{Rd.c} \cdot k_{rr} \cdot \left(100 \cdot \rho_{rr} \cdot f_{ck}\right)^{\frac{1}{3}} \right] \cdot b_{w.rr} \cdot d_{z.hr} \, MPa = 436.882 \cdot kN$$

$$v_{min.rr} := \left(0.035 \cdot k_{rr}^{\frac{3}{2}} \cdot \sqrt{f_{ck}} \right) \cdot \left(b_{w.rr} \cdot d_{z.hr}\right) \cdot 1 MPa = 256.215 \cdot kN$$

So OK!

Punching shear resistance according to EC2

For punching shear the average depth flexural depth of the slab is used as in the case of one way shear

$d_{z.hr} = 0.227\,m$

Perimeter of the critical section for punching

Calculate reinforcement ratio in both x and y direction

For bars lying along the x-axis

$$A_{steel.x.rr} := \frac{A_{steel.total.top}}{L_{slab}} \cdot \left(c_1 + 2 \cdot 3 \cdot d_{z.hr}\right) = 5.274 \times 10^{-3}\, m^2$$

According to EC2 section 6.4.4, the reinforcement is taken at a distance of c+3d on each side

$$\rho_{y.rr} := \frac{A_{steel.x.rr}}{d_{z.hr} \cdot 1m} = 0.023$$

For bars lying along the y-axis

$$\rho_{x.rr.1} := \frac{A_{steel.total.2}}{L_{slab.2}} \cdot \left(c_1 + 2 \cdot 3 \cdot d_{z.hr}\right) = 1.321 \times 10^{-3}\, m^2$$

$$\rho_{x.rr} := \frac{\rho_{x.rr.1}}{d_{z.hr} \cdot 1m} = 5.818 \times 10^{-3}$$

$$\rho_{2.rr} := \sqrt{\rho_{x.rr} \cdot \rho_{y.rr}} = 0.012$$

Control perimeter for punching shear

$$l_{1.rr} := c_1 + 0.9m + 4.d_{z.hr} = 2.108\,m$$

The perimeter of punching shear is taken for the case where load is close to the edge according to EC2. Perimeter is taken as 2d from each side

$$l_{2.rr} := 1.48m + 2 \cdot d_{z.hr} + \frac{c_1}{2} = 2.084\,m$$

$$u_{rr} := 2 \cdot l_{2.rr} + l_{1.rr} = 6.276\,m$$

$$V_{Rd.punching.rr} := \left[C_{Rd.c} \cdot k_{rr} \cdot \left(100 \cdot \rho_{2.rr} \cdot f_{ck}\right)^{\frac{1}{3}}\right] \cdot \left(u_{rr} \cdot d_{z.hr}\right) \cdot MPa = 1.192 \times 10^{3} \cdot kN$$

Moment resistance for higher reinforcement ratio

Determine the depth of the concrete block

$b = 1\,m$

$d_{rr} := d_{z.hr}$ Use an average value for the effective depth

Assume value of concrete cover on either side of 30mm

$cover_{rr} := 0.03m$

$spacing_{low} := spacing_{bar.top.x}$

$spacing_{low.2} := spacing_{bar.bottom.x}$

$$A_{s.1.rr} := \frac{\frac{\pi \cdot Dia_{bar.top.x}^{2}}{4} \cdot \left(\frac{L_{slab}}{spacing_{low}} + 1\right)}{L_{slab}} \cdot 1m = 3.173 \times 10^{-3}\,m^{2}$$ Top transversal reinforcement

$$A_{s2.rr} := \frac{\frac{\pi \cdot Dia_{bar.bottom.x}^{2}}{4} \cdot \left(\frac{L_{slab}}{spacing_{low.2}} + 1\right)}{L_{slab}} \cdot 1m = 2.701 \times 10^{-3}\,m^{2}$$ Bottom reinforcement

Assuming that the tension steel yields:

$\varepsilon_{s1} = 2.575 \times 10^{-3}$ Yield strain top tensile reinforcement

$$centroid_{rr} := \frac{cover \cdot A_{s.1.rr} + \frac{d_{rr}}{2} \cdot \left(b \cdot d_{rr}\right) + \left(d_{rr} - cover\right) \cdot A_{s2.rr}}{A_{s.1.rr} + d_{rr} \cdot b + A_{s2.rr}} = 0.113\,m$$ Centroid of the section

$$\varepsilon_{s.2.rr} := 0.003 \frac{\left(d_{rr} - centroid_{rr} - cover\right)}{\left(d_{rr} - centroid_{rr}\right)} = 2.208 \times 10^{-3}$$ Less than yield strain, bottom reinforcement

$\sigma_{compression.steel.rr} := \varepsilon_{s.2.rr} \cdot E_s = 441.646 \cdot MPa$ Less than yield stress of 515 MPa

$a_{rr} := \frac{\left(\left(A_{s.1} \cdot f_y - A_{s2} \cdot \sigma_{compression.steel.deep}\right)\right)}{0.85 \cdot f_{ck} \cdot b \cdot MPa} = 0.02\,m$ Height of concrete compression block

$\sigma_{tension.steel} = 515 \cdot MPa$

Concrete-steel and steel-steel couple used to give the resistance

$m_{y.top.rr} := \left(\sigma_{tension.steel} \cdot A_{s.1.rr} - \sigma_{compression.steel.rr} \cdot A_{s2.rr}\right)\left(d_{rr} - \frac{a_{rr}}{2}\right) \ldots = 295.016 \cdot kN \cdot m$
$+ \sigma_{compression.steel.rr} \cdot A_{s2.rr} \cdot \left(d_{rr} - 2cover\right)$

$Dia_{bar.rr} := 0.012m$

$A_{steel.rr.x.1} := \frac{\frac{\pi \cdot Dia_{bar.rr}^{2}}{4} \cdot \left(\frac{L_{slab.2}}{spacing_{low.2}} + 1\right)}{L_{slab.2}} \cdot 1m = 1.549 \times 10^{-3}\,m^2$

Now top reinforcement in x direction:

Centroid of the section

$centroid_{x.rr} := \frac{cover \cdot A_{steel.rr.x.1} + \frac{d_{rr}}{2} \cdot \left(b \cdot d_{rr}\right) + \left(d_{rr} - cover\right) \cdot A_{steel.rr.x.1}}{A_{steel.rr.x.1} + d_{rr} \cdot b + A_{steel.rr.x.1}} = 0.114\,m$

$\varepsilon_{s.2.x.rr} := 0.003 \frac{\left(d_{rr} - centroid_{x.rr} - cover\right)}{\left(d_{rr} - centroid_{x.rr}\right)} = 2.207 \times 10^{-3}$ Less than yield strain, bottom reinforcement

$\sigma_{compression.steel.x.rr} := \varepsilon_{s.2.x.rr} \cdot E_s = 441.41 \cdot MPa$ Less than yield stress of 515 MPa

Height of concrete compression block

$$a_{2.rr} := \frac{\left(\left(A_{steel.rr.x.1} \cdot f_y - A_{steel.rr.x.1} \cdot \sigma_{compression.steel.x.rr}\right)\right)}{0.85 \cdot f_{ck} \cdot b \cdot MPa} = 3.352 \times 10^{-3}\,m$$

Concrete-steel and steel-steel couple used to give the resistance

$$m_{x.top.rr} := \begin{pmatrix} \sigma_{tension.steel.deep} \cdot A_{steel.rr.x.1} \cdots \\ +-\sigma_{compression.steel.x.rr} \cdot A_{steel.rr.x.1} \\ +\left[\sigma_{compression.steel.x.rr} \cdot A_{steel.rr.x.1} \cdot \left(d_{rr} - 2cover\right)\right] \end{pmatrix} \cdot \left(d_{rr} - \frac{a_{2.rr}}{2}\right) \ldots = 139.838 \cdot kN \cdot m$$

$$m_{x.bottom.rr} := m_{x.top.rr}$$

$$m_{y.bottom.rr} := m_{x.bottom.rr}$$

YIELD LINE METHOD

Assume a value for the displacement under the point load is taken as 1m

$$b_{yield} = 1.2\,m$$

$$a_{load} = 1.3\,m$$

$$L_{slab.2} = 2.78\,m$$

$$f_{slab} := a_{load} \cdot \tan(10deg) = 0.229\,m$$

$$e_{slab} := a_{load} \cdot \tan(32deg) = 0.812\,m$$

$$c_{slab} := a_{load} \cdot \tan(32deg) = 0.812\,m$$

Yield line number 1:

$$yield_{one.rr} := m_{y.top.rr} \cdot b_{yield} \cdot \frac{1}{a_{load}} = 272.323 \cdot kN \cdot m$$

Yield line number 2:

$$yield_{two.rr} := 2 \cdot m_{x.top.rr} \cdot L_{slab.2} \cdot \frac{1}{c_{slab}} + 2 \cdot m_{y.top.rr} \cdot e_{slab} \cdot \frac{1}{a_{load}} = 1.326 \times 10^{3} \cdot kN \cdot m$$

Yield line number 3:

$$yield_{three.rr} := 2 \cdot m_{x.bottom.rr} \cdot a_{load} \cdot \frac{1}{c_{slab}} + 2 \cdot m_{y.bottom.rr} \cdot f_{slab} \cdot \frac{1}{a_{load}} = 496.891 \cdot kN \cdot m$$

$$Load_{flexure.rr} := \frac{yield_{one.rr} + yield_{two.rr} + yield_{three.rr}}{1m} = 2.095 \times 10^{3} \cdot kN$$

LEVEL III ANALYSIS

One-way shear resistance for high reinforcement ratio

$d_{3.hr} := 0.38m - 0.03m - 0.028m = 0.322\,m$ — d is the effective depth at the maximum depth section

$d_{z.hr} = 0.227\,m$ — Average effective depth

$z_{hr} := d_{z.hr} - 0.03m - 0.02m + 0.008m = 0.185\,m$ — Distance between reinforcements, so furthur subtract cover

$$k_{v.hr} := \frac{180mm}{1000mm + 1.25 \cdot z_{hr}} = 0.146$$

$d_{cr.hr} := 1.3m - d_{3.hr} = 0.978\,m$

$b_{w.hr} := 0.9m + 2 \cdot d_{cr.hr} \cdot \tan(45deg) + 0.3m = 3.156\,m$ — Location of the critical section

$b_{w.hr} = 3.156\,m$

$$V_{Rd.c.shear.hr} := k_{v.hr} \cdot \frac{\sqrt{f_{ck}} \cdot MPa}{\gamma_c} \cdot z_{hr} \cdot b_{w.hr} = 359.893 \cdot kN$$

According to the new proposed method

$$V_{Rd.c.shear.hr.pm} := k_{v.hr} \cdot \frac{\sqrt{f_{ck}} \cdot MPa}{\gamma_c} \cdot z_{hr} \cdot 2.1m = 239.473 \cdot kN$$ The control section is taken at a distance of min (d, a/2) from the support.

Punching shear resistance high reinforcement ratio

$d_{z.hr} = 0.227\,m$

Perimeter of the control section calculated at a distance of 0.5d from the support

$l_{hr.1} := 0.9m + c_1 + d_{z.hr} = 1.427\,m$

$l_{hr.2} := c_1 + 0.5 \cdot d_{z.hr} = 0.413\,m$

$b_{0.hr.1} := 2 \cdot l_{hr.2} + l_{hr.1} = 2.254\,m$

2.4 EDGE BEAMS

The capacities are taken as the same as the reference model for all three levels of analysis

Appendix C - Mean Crack Distance

X Direction (12ϕ@150mm)

The neutral axis is considered in the middle of the section as the amount of reinforcement in the x direction is the same in the bottom and the top layer of the slab

$\phi_x := 12mm$ Diameter of bar in x direction

$s_x := 150mm$ Bar spacing in x direction

$b := 1m$ unit width

$n_x := \frac{b}{s_x} = 6.667$ Number of bars

$t_m := \frac{(0.38 + 0.19)m}{2} = 0.285\,m$ Mean thickness of slab

$x := \frac{t_m}{2} = 0.143\,m$ Neutral axis

$c := 30mm$ Cover

$k_1 := 0.8$

$k_2 := 0.5$

$k_4 := 0.425$

$d := t_m - (30 + 12 + 6)mm = 0.237\,m$ Effective depth

$h_{ef} := \min\left[2.5\cdot(t_m - d), \frac{(t_m - x)}{3}, \frac{t_m}{2}\right] = 0.048\,m$

$A_{c.x} := b\cdot h_{ef} = 0.048\,m^2$

$A_{sx} := n_x\cdot\frac{\pi\cdot\phi_x^{\,2}}{4} = 7.54\times 10^{-4}\,m^2$

$\rho_x := \frac{A_{sx}}{A_{c.x}} = 0.016$

$s_{rmax.x} := 3.4\cdot c + 0.425 k_1\cdot k_2\cdot\frac{\phi_x}{\rho_x} = 0.231\,m$

Y direction 14ϕ@75mm

$d_1 := 1m \qquad d_2 := 1m$ Intial Assumption

Given

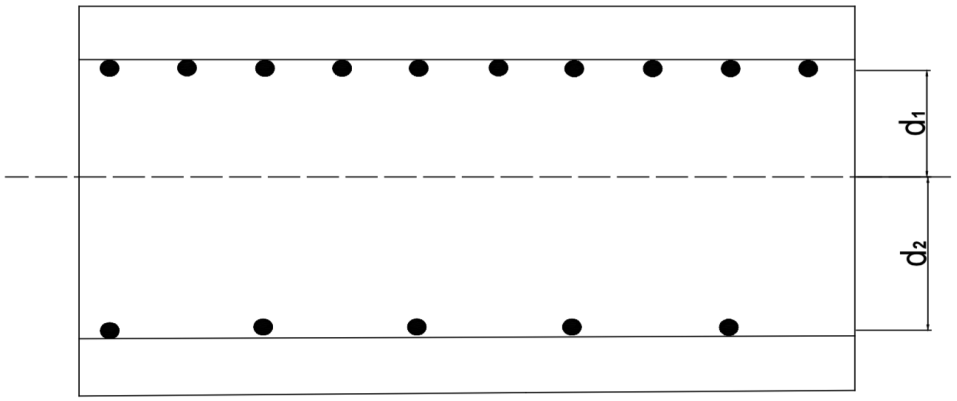

$s_y := 75mm$ Bar spacing in y direction

$n_y := \frac{b}{s_y} = 13.333$ Number of bars

$\phi_y := 14mm$ Diameter of bars in y direction

$n_x = 6.667$

Calculation of neutral axis

$d_1 \cdot \phi_y \cdot n_y = d_2 \cdot \phi_x \cdot n_x$

$d_1 + d_2 = \left(t_m - 2 \cdot c - \frac{\phi_x}{2} - \frac{\phi_y}{2} \right)$

$\text{Find}(d_1, d_2) = \begin{pmatrix} 0.064 \\ 0.148 \end{pmatrix} m$

$d_y := t_m - 0.064m - \frac{\phi_y}{2} = 0.214\,m$

$h_{efy} := \min\left[2.5(t_m - d), \frac{(t_m - d_y)}{3}, \frac{t_m}{2} \right] = 0.024\,m$

$b = 1\,m$

$A_{cy} := b \cdot h_{efy} = 0.024\,m^2$

$$A_{sy} := n_y \cdot \frac{\pi \cdot \phi_y^{\,2}}{4} = 2.053 \times 10^{-3}\,\mathrm{m}^2$$

$$\rho_y := \frac{A_{sy}}{A_{cy}} = 0.087$$

$$s_{rmax.y} := 3.4 \cdot c + 0.425 k_1 \cdot k_2 \cdot \frac{\phi_y}{\rho_y} = 0.129\,\mathrm{m}$$

$$s_{rmax} := \frac{1}{\frac{\cos(0)}{s_{rmax.y}} + \frac{\sin(0)}{s_{rmax.x}}} = 0.129\,\mathrm{m}$$

$$s_{rmean} := \frac{s_{rmax}}{1.7} = 0.076\,\mathrm{m}$$

Appendix D- Deflection under self weight

$\gamma_{conc} := 25\frac{kN}{m^3}$ Reinforcement density

$b := 1m$ Unit breadth

$l := 2.78m$ Length

$E := 36GPa$ Youngs modulus

$t_m := \frac{(0.38 + 0.19)}{2}m = 0.285\,m$ Mean thickness

$g := \gamma_{conc} \cdot b \cdot t_m = 7.125 \cdot \frac{kN}{m}$ Self-weight

$I_m := \frac{b \cdot t_m^{\,3}}{12} = 1.929 \times 10^{-3}\,m^4$

$\delta_{free} := \frac{g \cdot l^4}{8 \cdot E \cdot I_m} = 7.66 \times 10^{-4}\,m$ Deflection at free end

The deflection calculated assumes a cantilever beam with uniform cross sectional area. In reality, the beam has a constanlty varying cross section area.The inertia and the centroid becomes a function of the span which is not reflected in the simplified calculation shown above. It is expected that the value for deflection is over estimated in this case.